Title

Hydrological regime and plant functional traits jointly mediate the influence of *Salix* spp. on soil organic carbon stocks in a High Arctic tundra

Title shortened version

Plant and environmental drivers of soil carbon stocks

Authors

Laurent J. Lamarque[1,2,*], Jim Félix-Faure[1], Lucas Deschamps[1], Esther Lévesque[1,2], Pier-Olivier Cusson[1,3], Daniel Fortier[2,4], Matteo Giacomazzo[5], François Guillemette[1], Jennifer Paillassa[1,2], Maxime Tremblay[1], Vincent Maire[1,2]

[1]Département des Sciences de l'environnement, Université du Québec à Trois-Rivières, Trois-Rivières, QC, Canada; [2]Centre d'études nordiques, Université Laval, Québec, QC, Canada; [3]Département de biologie, Université de Sherbrooke, Sherbrooke, QC, Canada; [4]Département de géographie, Université de Montréal, Montréal, QC, Canada; [5]Department of biology, University of New Brunswick, Fredericton, NB, Canada

*Corresponding author: Laurent J. Lamarque. E-mail: llamarqueab@gmail.com

Author contributions

LJL, EL and VM conceived and designed the research. LJL, EL and MT collected the material. LJL and P-OC processed soil samples prior to analyses. LJL, EL, FG and VM supervised soil analyses. LJL, JFF, LD, VM and MG analyzed data. LJL and VM led the writing of the manuscript, with contributions of all co-authors.

Abstract

Evidence points out that increasing plant productivity associated with greater erect shrub abundance alters soil organic carbon (SOC) stocks in the Arctic. However, the underlying plant economic traits remain poorly examined, which limits our understanding of plant-environment interactions driving tundra carbon cycling. We explored how erect shrub abundance leads to SOC variation in a High Arctic tundra (Bylot Island, Nunavut, Canada), where the only erect shrub, *Salix richardsonii*, has settled along currently active and abandoned channel zones of alluvial fans. The effects of vegetation and local environmental changes on SOC were evaluated through a paired sampling of soil materials and plant aboveground functional traits associated with plant carbon supply and nutrient demand processes. The occurrence of *S. richardsonii*, characterized by a 10-fold increase in aboveground biomass, induced a 28% increase in SOC compared to adjacent plots dominated by prostrate shrubs and graminoids. Yet, this vegetation effect was solely observed along active channels, where higher SOC was associated with greater leaf and stem biomass. A path analysis showed that shrub leaf area index and total leaf nutrient content best represented plant carbon supply and nutrient demand dynamics, respectively, and jointly regulated SOC variation. This study underscores that vegetation structural changes associated with increasing erect shrub abundance in the Arctic can promote soil organic carbon storage, but that this pattern may be mediated by strong plant-environment interactions. Accounting for changes in functional traits driving plant carbon supply and nitrogen demand proves important for a better mechanistic understanding of how shrubification impacts tundra carbon cycling.

Key words

Alluvial fan; Carbon supply; Leaf area index; Nutrient demand; Plant-enhanced mineralization; Shrubification.

Manuscript highlights

- Increasing erect shrub abundance along High Arctic alluvial fan channels can lead to increasing soil organic carbon stocks
- Fine-scale interactions between hydrological regime and vegetation conditions regulate changes in soil organic carbon stocks
- Plant traits associated with carbon supply and nutrient demand may provide new insights on carbon cycling variation with vegetation shifts

Introduction

The greening of tundra ecosystems, mainly driven by the significant increase in erect shrub height (Bjorkman and others 2018), biomass and canopy cover (Myers-Smith and others 2011; Elmendorf and others 2012), has been a major component of the vegetation changes observed in the Arctic over the past few decades of global warming (Epstein and others 2013; Myers-Smith and others 2020). Rapid erect shrub expansion (c.f. shrubification) at the expense of non-vascular and herbaceous vegetation has been initially expected to increase soil organic carbon (SOC) stocks (Myers-Smith and others 2011), as plant carbon supply to soils is proportional to primary productivity (Metcalfe and others 2018; Chen and others 2021), and decomposition of shrub leaf litter is slower than that of forbs and grasses (Cornelissen and others 2007). Models developed to estimate variation in ecosystem carbon balance with vegetation changes in northern latitudes have notably pointed towards this scenario (Qian and others 2010; Mekonnen and others 2018). Yet, greater erect shrub abundance has not necessarily increased soil organic carbon stocks (Parker and others 2021), which in various sites have even been lower beneath shrub-dominated communities than beneath adjacent heaths, meadows or tussock tundra (Wilmking and others 2006; Sørensen and others 2018). A better understanding of the common

mechanisms driving the fate of assimilated carbon in the wake of Arctic vegetation changes is thus needed, especially to bolster estimation of future Arctic ecosystem carbon storage.

Changes in tundra carbon stocks and cycling with greater erect shrub abundance can first be associated with shifts in plant-regulated soil microclimate and microbial community (Wallenstein and others 2007; Myers-Smith and Hik 2013; Kemppinen and others 2021; relation 1 in Figure 1). Two plant-induced processes can also occur concurrently: a significant increase in fresh energy-rich carbon supply (referred hereafter as plant carbon supply) with increasing litter quality and quantity (DeMarco and others 2014; Liang and others 2018; relation 2 in Figure 1), and a loss of recalcitrant energy-poor soil organic matter (SOM) to the atmosphere following plant-enhanced mineralization (c.f. positive priming; Fontaine and others 2011; relation 3 in Figure 1). Thus, the long-term plant regulation of the net SOC balance is linked to the maintenance of the carbon-nutrient stoichiometry required for optimal plant metabolism (Zhen 2009; Maire and others 2013; relation 4 in Figure 1).

Plant-enhanced mineralization (i.e. positive priming) is a key process to determine long-term sequestration of carbon (C) and nutrient (N) in SOM (c.f. 'bank mechanism'; Fontaine and Barot 2005; Perveen and others 2014). This process is regulated by the availability of nutrients in soil solution, and ultimately by plant N uptake (Fontaine and Barot 2005; Perveen and others 2014). Under conditions where plant N demand is lower than soil N supply, soil microbes are prone to sequester N in SOM through microbial immobilization (Martel and Paul 1974), and plant-enhanced mineralization is rather low. This eventually leads to new SOM humification and strong soil C gain (Loya and others 2002; Kallenbach and others 2016). The fate of carbon stored in the soil then depends on how plant-derived C is efficiently fragmented and/or incorporated into microbial products and stabilized on minerals (Cotrufo and others 2015).

In contrast, under conditions where plant N demand overcomes soil N supply, plant litter and photosynthate-C allocation to the rhizosphere enhance respiration of C-limited microbial communities, which in turn promote the degradation of recalcitrant nutrient-rich SOM and the release of mineral nutrients that become available for plants (Dijkstra and others 2009, 2013; Huo and others 2017). SOM microbial mining is thus related to plant N demand (Perveen and others 2014; Henneron and others 2020b), which is closely linked to plant nutrient uptake (Kou and others 2022). This process can at times be so important that it exceeds the formation of new SOM through humification of fresh C (Fontaine and others 2004; Terrer and others 2021), leading to soil C loss. To date, studies on soil functioning in tundra ecosystems, where plant growth is generally limited by low nutrient availability (e.g. phosphorus and nitrogen in Elser and others 2007), have highlighted both microbial N-limitation on SOC decomposition rates (Sistla and others 2012) and SOM degradation of N-rich SOM in many sites (Keuper and others 2020). However, the extent to which particular functional traits associated with plant physiology and/or size drive plant N demand and SOM microbial mining has received less attention. This currently limits our understanding of how plant-environment interactions shape tundra carbon cycling, especially in the context of Arctic shrubification.

Meanwhile, other investigations have indicated also that plant species identity (Lynch and others 2018; Street and others 2020; Gavazov and others 2022), therefore different N-acquisition strategies, are key drivers of tundra soil organic carbon dynamics (Hewitt and others 2019; Clemmensen and others 2021). Rates of plant nutrient demand and carbon supply are tightly linked to the leaf economics spectrum, contrasting resource acquisitive with conservative species (Henneron and others 2020a, b). Acquisitive species characterized by high leaf N content and high metabolic activity are more prone to stimulate SOM mining, whereas conservative species with low leaf N and low metabolic activity are more likely to induce new SOM humification (Henneron and others 2020b; Clemmensen and others 2021). Across the

tundra biome, plant communities have been subjected to a strong turnover of species marked by the arrival of acquisitive species such as erect shrubs exhibiting high leaf nitrogen and high specific leaf area (Bjorkman and others 2018). This pattern has nonetheless been strongly associated with wetter habitats, as erect shrub expansion appears to be constrained by limited soil moisture availability (Myers-Smith and others 2015). Conservative species would thus be expected to dominate in drier habitats. However, tundra vegetation has also the potential to respond plastically to environmental changes (Bret-Harte and others 2001; Hudson and others 2011), and acquisitive species might be able to colonize a wide range of environments. Within-species variation in organic carbon stored in shrub biomass across environments has not yet been comprehensively quantified (relations 7 & 8 in Figure 1). This hampers our understanding of the extent of shrub control over soil organic carbon stocks across environmental conditions and how it would evolve if growing conditions improve.

This study aimed at determining the extent to which erect shrub abundance and environmental changes modulate long-term soil organic carbon stock dynamics in Arctic tundra ecosystems. Our work centered around *Salix richardsonii* Hook. at the northern edge of its distribution range, in a High Arctic alluvial fan landscape where it is the only erect shrub species encountered. The influence of environmental changes was examined by contrasting zones with different hydrological regime and sediment input intensity, where *S. richardsonii* occurs in patches and is expected to display variation in traits associated with C supply and N demand. Specifically, we used an observational approach to evaluate how SOC stocks vary as a function of vegetation (i.e. presence/absence of *S. richardsonii*) and hydrological regime (i.e. active vs. abandoned channels).

Materials and methods

Study area

141 The study took place in the Qarlikturvik valley of Bylot Island, Nunavut, Canada (73°09'N,
142 79°57'W; Figure 2a). At the altitude of 20 m a.s.l, the mean total annual precipitation is 220
143 mm (snow and rain), while the mean annual temperature and mean temperature of the warmest
144 month (July) are -15°C and 6.1°C, respectively (Gauthier and others 2013). This 122 km^2 valley
145 connects C-79 and C-93 glaciers to the Navy Board Inlet sea via a proglacial river (Coulombe
146 and others 2022). It is mainly characterized by a low-centered polygon landscape (Fortier and
147 Allard 2004) that is composed of wetlands dominated by grasses and sedges, and mesic
148 environments that harbour a greater species richness including prostrate shrubs like *Salix*
149 *arctica*, *Salix reticulata* and *Salix herbacea* (Gauthier and others 2013; Perreault and others
150 2016). The valley is bounded to the North and South by plateaus of ~400 m made of poorly-
151 consolidated shale and sandstone (Miall and others 1980). After deglaciation, stream incision
152 and gullying in the plateaus formed alluvial fans at the base of the valley walls (Fig. 2a; Blair
153 and McPherson 2009). These alluvial fans are grossly conical in shape, with a narrow apex, an
154 arcuate frontal section, and a convex cross-section. They correspond to aggradational
155 sedimentary deposits gradually widening with time, and comprise surface channels which
156 receive sediment and nutrients from upslope throughout the plant growing season, migrate
157 laterally with sedimentation, and can become temporarily or permanently abandoned (Rioux
158 2021).

159 **Study design**

160 Fieldwork was carried out on 4-6 July 2015 along two alluvial fans located at the foot of the
161 valley southern plateau (Figure 2a), and that were randomly selected from the fifteen fans along
162 which *Salix richardsonii* occurs. Observations along each fan were conducted in two zones
163 with contrasting hydrological regime and sediment input intensity: (i) active channels, where
164 water flows yearly and sediment input is greater, and (ii) abandoned (i.e. inactive) channels,
165 where water doesn't flow anymore and vegetation colonizes the bed of these channels (Figure

166 2b). Along each channel, a paired sampling was carried out in two vegetation conditions, that
167 were ca. 3-5 m apart and defined by the absence or dominance of *Salix richardsonii* (c.f.
168 'outside/beneath *SR*' in Figure 2c). Three pairs of quadrats were randomly chosen along each
169 channel, leading to a total of 24 experimental units (i.e. 2 alluvial fans x 2 channels x 3 paired
170 replicas). At these locations, the height of *S. richardsonii* individuals averaged 35 ± 2 cm, with
171 no difference in height between channels (F = 1.0, P = 0.99). A preliminary
172 dendrochronological study of largest branches showed that these individuals are at least 100-
173 year-old (Bisson 2016).

174 **Vegetation characterization and woody plant trait measurements**

175 Species richness and abundance were determined in each randomly deployed pair of 0.7 m x
176 0.7 m quadrats. Abundance of woody and graminoid species, lichens and mosses were
177 quantified using Daubenmire cover abundance classes (Daubenmire 1959). Aboveground
178 biomass of woody and graminoid species was also measured, within a 0.2 m x 0.2 m quadrat
179 set up at the bottom left corner of each 0.7 m x 0.7 m quadrat. Leaves were separated from
180 stems for each of the three woody species encountered in these sites, namely *Salix richardsonii*,
181 *S. arctica* and *S. reticulata*. Biomass samples were oven-dried at 65°C for a minimum of 72
182 hours and weighed after drying.

183 Prior to plant collection, a picture was taken at a height of 1.50 m above each 0.2 m x 0.2 m
184 quadrat to determine the total number of leaves of each of the three *Salix* species. A subsample
185 of 3-20 leaves per *Salix* species per quadrat was additionally separated and stored in a plastic
186 bag at 4°C until leaf area (cm^2) was estimated back at the camp facilities using WinFOLIA
187 software (Regent Instruments Inc, Quebec City, QC, Canada). These leaf samples were also
188 oven-dried at 65°C for a minimum of 72 hours and weighed after drying. The following leaf
189 traits were measured per *Salix* species per quadrat: leaf size (cm^2 leaf), leaf dry mass (DM, g),
190 and leaf composition in C, N, P, K, Ca, Mg, $\delta^{13}C$ and $\delta^{15}N$. Elementary chemical analyses (leaf

C, N, P, K, Ca, Mg content) were performed using inductively coupled plasma-atomic emission spectroscopy (Plasma Model 40, PerkinElmer, Waltham, MA, USA) following a Mehlich-3 acid extraction method. Leaf $\delta^{13}C$ and $\delta^{15}N$ isotopic composition was determined using an elemental analyzer coupled with an isotope ratio mass spectrometer (EA-IRMS, Agilent technology, Santa Clara, CA, USA).

For each *Salix* species, specific leaf area (SLA, cm^2 leaf g^{-1} DM) was calculated as the ratio of leaf area to leaf dry mass; leaf area index (LAI_w, m^2 leaf m^{-2} soil), as the ratio of total leaf area (i.e. leaf size x total number of leaves in the quadrat) to corresponding quadrat area; total leaf nutrient content (TLN_w, kg m^{-2} soil), as the product of leaf nutrient content ($LNuC_w$; i.e. the cumulative leaf content in N, P, K, Ca and Mg) and leaf biomass. Community-weighted trait means (that is, the mean trait value of *Salix* species weighted by the abundance of each species) were calculated per quadrat for each functional trait aforementioned.

Soil sampling and analyses

Within each quadrat, three soil cores were collected using a 15-cm long and 6-cm diameter corer. When present, the moss layer (0-5.8 cm deep) was immediately separated and stored in a paper bag. Moss biomass was oven-dried at 65°C for a minimum of 72 hours and weighed after drying. Soil cores were extracted down to the thaw front depth at the date of sampling. They systematically exceeded the root front and had a total depth (i.e. depth of the thawed portion of soil) ranging between 6.7 and 9.2 cm without moss layer. Upon soil core extraction, two soil horizons were distinguished visually using the Canadian System of Soil Classification, and immediately separated: A_1, which corresponded to the upper 1.8 ± 0.3 cm (mean ± SE), and contained the majority of fine roots; and A_2, corresponding to the next 5.8 ± 0.2 cm, and that was weakly colonized by roots (Figure 1c). For each quadrat, the three soil core replicates were pooled per soil horizon, and stored in plastic bags at 4°C.

Back in the laboratory, fresh soil samples were weighed, and air-dried at 25°C. They were then sieved at 2 mm to separate roots from coarse organic material (> 2 mm), and fine earth (< 2 mm, M_t). Coarse organic material and fine earth were then weighed separately. Root biomass was oven-dried at 65°C for a minimum of 72 hours, and weighed after drying. A first aliquot of ~10 g of fine earth was oven-dried at 105°C to determine water content (in %) as follows: ((fresh weight-dry weight)/dry weight)*100. A second aliquot of ~30 g of fine earth was oven-dried at 60°C until constant weight (M_{od}), and the following parameters were measured: pH in soil water; particle-size distribution, using a laser particle-size analyser (Laser Particle Sizer Analysette 22 MicroTec Plus, Fritsch, Idar-Oberstein, Germany); soil organic C and N content, after decarbonation by HCl fumigation; soil $\delta^{13}C$ and $\delta^{15}N$ isotopic composition, using the same methodology than for leaf $\delta^{13}C$ and $\delta^{15}N$ (see above).

The remainder of fine earth (12.8-33.5 g of soil air-dried at 25°C, and < 2 mm) was successively wet-sieved for two minutes at 1 mm, 250 µm and 63 µm to differentiate the particulate organic matter compartments (POM) as follows: coarse organic matter (cPOM, 2 mm to 1 mm), medium organic matter (mPOM, 1 mm to 250 µm) and fine organic matter (fPOM, 250 µm to 63 µm), respectively. Each of the sieved fractions was dried in an oven at 60°C until a constant weight was obtained, weighed with a precision of ± 0.0001 g (M_{ad} compartments: M_{ad_cPOM}, M_{ad_mPOM}, M_{ad_fPOM}), and then analyzed to obtain total soil organic C and total N content, as well as soil ^{13}C and ^{15}N isotopic composition. The C content of the mineral-associated OM (MAOM; Lavallee and others 2020) was subsequently estimated as the difference between SOC_{tot} and the C contained in the three measured POM compartments.

Finally, composite samples of cPOM, mPOM and fPOM from the A_2 horizon were used for all sites (12 samples in total) to analyze radiocarbon (^{14}C) composition at the A.E. Lalonde AMS laboratory (University of Ottawa, Canada), following protocols detailed in Crann and others (2017). The fraction modern carbon, $F^{14}C$, was calculated as the ratio of the sample

240 $^{14}C/^{12}C$ to the standard $^{14}C/^{12}C$ ratio (here Ox-II) measured in the same data block, and the
241 result was normalized to $\delta^{13}C$ (PDB) following correction for spectrometer and preparation
242 fractionation. The $D^{14}C$ was calculated as ($F^{14}C$-1)*1000, and the $\Delta^{14}C$ as ($F^{14}C$*e(1950-
243 y)/8267)-1)*1000 (Crann and others 2017).

244 **Quantifying soil organic carbon stocks**

245 The volumetric carbon content C_{vol} (gC m^{-3} soil) of fine earth and POM compartments was first
246 calculated per quadrat as follows:

247 $$C_{vol} = \frac{M_t}{M_{ad}} \cdot M_{od} \cdot C \cdot \frac{1}{V} \quad \text{Eq. 1}$$

248 where M_{od} (g) refers to the weight of the oven-dried aliquot of fine earth (see above), C (g g^{-1}
249 soil) is the total organic carbon content of the corresponding soil sample, and V (m^{-3}) is the
250 soil bulk volume that was calculated from the diameter of the corer and the length of each of
251 the three soil cores sampled per quadrat and pooled per soil horizon. The ratio M_t/M_{ad} was used
252 to account for the weight of POM compartments (M_{ad}) compared to the total air-dried weight
253 of fine earth (M_t). Soil bulk volume included coarse elements which contributed marginally to
254 soil C content. Coarse elements were present in 64% of the soil samples, and when present
255 accounted for only 2% of soil bulk volume, with no difference between vegetation conditions
256 and channel zones ($P > 0.33$ in both cases).

257 The surfacic (i.e. area based) carbon content C_{surf} (gC m^{-2} soil) of fine earth and POM
258 compartments was calculated as follows:

259 $$C_{surf} = \frac{M_t}{M_{ad}} \cdot M_{od} \cdot C \cdot \frac{1}{S} \quad \text{Eq. 2}$$

260 where S (m^2) is the soil surface that was obtained from the diameter of the corer.

261 **Soil temperature monitoring**

Soil temperature was assessed with HOBO Pendant 64K data loggers (Onset Computer Corporation, Bourne, MA, USA; accuracy of ± 0.53°C from 0° to 50°C, resolution of 0.14°C at 25°C), that were deployed in three paired vegetation conditions (outside and beneath *S. richardsonii*) along one of the two alluvial fans studied (1 fan x 2 channels x 3 paired replicas = 12 loggers). Each logger recorded soil temperature at 6 cm depth hourly during one year between July 2017 and July 2018. Freezing degree-days (FDD) were calculated as the cumulative sum of daily average negative temperatures between summer 2017 and summer 2018, while thawing degree-days (TDD) were calculated as the cumulative sum of daily average positive temperatures for the years 2017 and 2018.

Statistical analyses

Testing the effect of hydrological regime and Salix richardsonii occurrence on plant communities and soil conditions - We first ran linear mixed models (MIXED procedure with REML method in SAS 9.4, SAS Institute, Cary, NC) to explain variation in plant traits, soil conditions and SOC with changes in hydrological regime and occurrence of *S. richardsonii* . Channel (active vs abandoned), vegetation condition (outside vs beneath *S. richardsonii*), and the interaction between channel and vegetation condition were treated as fixed factors, with random effects structured as pairs of quadrats nested within channels within fans. We checked prior to analyses that the random effects were normally distributed. Evaluation of significant effects was based on an alpha of 0.05. As multiple comparisons were performed, the significance of results was further assessed using the False Discovery Rate procedure (Benjamini and Hochberg 1995; but see Pike 2011 for the method applied in ecology and evolution). In addition, we quantified (i) the association between plant community and soil conditions with a multivariate canonical correspondence analysis (CCA; ter Braak and Verdonschot 1995), and (ii) the association between channel, vegetation conditions, and leaf

nutrients of *Salix* spp. with a principal component analysis (PCA), using the *vegan* package in R version 4.0.4 (R Development Core Team 2021).

Testing the influence of plant carbon supply and nutrient demand on soil organic carbon stocks - This analysis was conducted using a two-step approach. First, we selected the measured community-weighted traits (i.e. variables) that were associated with C supply and N demand, and could best represent the influence of the two processes on soil organic carbon stock variation. Specifically, we used (i) SLA_w, LAI_w, and moss biomass as proxies of plant C supply, considering in particular that SLA_w and LAI_w are associated with plant fast resource acquisition and rapid growth (Wright and others 2004; Sterck and others 2011), and with gross and net primary productivity (Shaver and others 2013); (ii) leaf nutrient content ($LNuC_w$), leaf/stem/root biomass, and TLN_w as proxies of plant nutrient demand, considering that the biomass of leaves, stems and roots is directly related to the cost of tissue maintenance that requires soil nutrients (Givnish and others 2014). A multi-model inference that included the eight aforementioned explicative variables was performed to investigate the sources of variation in soil organic carbon stocks. We used the *MuMIn* package in R, and a linear mixed regression model with random effects structured as pairs of quadrats nested within channels within fans. We used model weights to estimate the relative importance of each variable under consideration (*dredge* function). We checked for model convergence (*nloptwrap* function), and used AICc as the ranking-based index. Then, we selected the most important variable for each of the carbon supply and nutrient demand process (*importance* function). The two selected variables were included in a path analysis that was performed based on the series of mixed regressions identified in Figure 1, using the *piecewiseSEM* package in R (Lefcheck 2016). Variation in SOC stocks was modelled with multiple linear mixed regression models (n = 24 experimental units; *nlme* package in R), using plant carbon supply, plant nutrient demand, hydrological regime and occurrence of *S. richardsonii* as fixed factors. Pairs of quadrats nested

311 within channels within fans were considered as random factors. Implied directed separations
312 were tested, and associated *P*-values used to compute the model goodness-of-fit.

313 *Testing the influence of plant carbon supply and nutrient demand on soil organic carbon*
314 *quality* - Signatures of soil $\delta^{13}C$, ^{14}C and $\delta^{15}N$ were used to estimate the change in SOC quality
315 that has resulted from variation in soil carbon gain and OM degradation associated with
316 vegetation change (i.e. occurrence of *S. richardsonii*). Given that SOC stocks in the Arctic
317 mainly come from large plant residues with relatively little microbial processing (see e.g. Prater
318 and others 2020), differences in soil bulk $\delta^{13}C$ observed between vegetation conditions were
319 expected to result from the input of newly formed plant litter that is depleted in $\delta^{13}C$ as a
320 consequence of the Suess CO_2 fertilization effect (Ehleringer and others 2000; Camino-Serrano
321 and others 2019). Thus, the abundance of *S. richardsonii* and related additional carbon supply
322 were assumed to decrease soil bulk $\delta^{13}C$ (i.e. leading to more negative values). We used soil
323 bulk ^{14}C to visually test how vegetation conditions modified the average age of SOC, with more
324 positive values indicating more recent SOC.

325 Conversely to carbon isotopes, there is a significant microbial discrimination against ^{15}N
326 during OM mineralization when microbial growth is C-limited (Dijkstra and others 2009). This
327 leads to excretion of depleted mineral N and accumulation of $\delta^{15}N$ in microbial biomass, which
328 ultimately increases soil bulk $\delta^{15}N$ values (Dijkstra 2009; Craine and others 2015).
329 Theoretically, enrichment of soil $\delta^{15}N$ might also originate from N losses through volatilization,
330 denitrification and N leaching; however, the effect of these N losses on soil $\delta^{15}N$ signature is
331 likely marginal as the substantial increase in plant biomass related to the occurrence of *S.*
332 *richardsonii* is expected to reduce these N losses. Soil bulk $\delta^{15}N$ values might also be modified
333 by (i) N fixation - in this case, while N-fixing leguminous species such as *Astragalus alpinus*
334 were rare in our sampling plots, $\delta^{15}N$ might tend to zero due to N fixation by diazotrophs present
335 on mosses (Rousk and others 2017); and (ii) arbuscular and ectomycorrhizal associations

established by *Salix* spp. (Dhillion 1994) - in this case, there may be a ^{15}N depletion in plants and ^{15}N enrichment in mycorrhizal fungi (Hobbie and Hobbie 2009), likely leading to a zero-sum for bulk soil $\delta^{15}N$.

The effects of plant carbon supply and nutrient demand on soil bulk $\delta^{13}C$ and $\delta^{15}N$ across soil horizons and OM compartments were tested with generalized linear mixed models, where soil horizons and OM compartments as well as their interaction terms with plant carbon supply and nutrient demand were treated as fixed factors, and pairs of quadrats as well as fans nested within channel as random factors.

Results

Variation in plant communities

There was no significant difference between active and abandoned channels in *S. richardsonii* abundance (non-significant channel effect; $P = 0.08$), plant species richness ($P = 0.72$), and plant community (Supplementary materials 1-3).

As expected, abundance of *S. richardsonii* was significantly greater in plots sampled beneath (> 50% cover) than in plots sampled outside (< 0.5%) the species' patches (significant vegetation effect; $P < 0.001$; Supplementary material 1). The difference in *S. richardsonii* abundance between vegetation conditions did not translate into a difference in plant species richness, which remained low (5-7 species) both beneath and outside the species' patches ($P = 0.08$; Supplementary material 1). However, we observed a change in plant community composition, with living mosses and vascular plant species such as *Astragalus alpinus*, *Arctagrostis latifolia*, *Dryas integrifolia*, *Salix artica* and *S. reticulata* occurring in plots located outside *S. richardsonii* patches (Supplementary material 3).

The CCA testing the association between plant community and soil conditions further showed that soil variables (i.e. thaw front depth, bulk density, water content, pH, FDD, TDD,

C:N ratio, and total N content), hydrological regime and vegetation conditions together explained 57% of the total variation in species abundance, with the first two axes retaining 32% and 9% of the total variation, respectively (Supplementary material 4).

Variation in plant traits

No differences in plant biomass-related traits were found between active and abandoned channels (non-significant channel effect; $P > 0.07$ in all cases), with the exception of moss biomass that was significantly greater in abandoned channel zones (Table 1).

Regardless of the hydrological regime, significant differences in plant traits were observed between vegetation conditions, with the exception of root and moss biomass (Table 1, Supplementary material 1). For instance, plant aboveground biomass ranged from 112 gDW m^{-2} soil in plots outside *Salix richardsonii* to 1416 gDW m^{-2} soil beneath the species' patches (significant vegetation effect; $P < 0.001$; Table 1, Supplementary material 5), and was driven by a 10 to 30 times greater aboveground biomass of *S. richardsonii* in plots beneath the species' patches ($P < 0.001$; Table 1). Aboveground biomass of graminoids was 2 to 5 times greater in plots outside *S. richardsonii* patches. Stem and leaf biomass of *S. richardsonii* were respectively 95% and 70% greater than that of *Salix arctica* and *S. reticulata* ($P < 0.001$ and $P = 0.009$, respectively; Table 1). *S. richardsonii* exhibited significantly more leaves, larger leaves, and lower SLA than the other two *Salix* species ($P < 0.001$ in all cases; Supplementary material 1). Thus, LAI_w and TLN_w beneath *Salix richardsonii* were respectively twice and three times as big as in plots outside *S. richardsonii* patches ($P < 0.001$ and $P = 0.006$, respectively; Table 1).

The interaction between hydrological regime and occurrence of *S. richardsonii* led to significant differences in LAI_w ($r^2 = 0.73$, $P < 0.01$ for all additive and interactive terms). The difference was particularly strong between vegetation conditions along active channels, where LAI_w values were very low in plots outside *S. richardsonii* patches (Table 1).

385 The PCA testing the association between channel, vegetation conditions and leaf nutrients
386 of *Salix* spp. showed that *Salix* leaves also discriminated strongly against plots differing in the
387 *S. richardsonii* occurrence (Table 1, Supplementary materials 1 and 4). For instance, leaves of
388 *S. richardsonii* exhibited significantly 4% lower C, 14% higher N, 16% lower C:N ratio, and
389 16% higher nutrient content ($LNuC_w$) compared to leaves of other *Salix* species found in plots
390 outside *S. richardsonii* patches (Supplementary material 1). No difference in leaf biochemistry
391 was observed between active and abandoned channels ($P > 0.16$ in all cases; Table 1,
392 Supplementary material 1).

393 **Variation in soil conditions**

394 At the time of sampling in early summer, some differences in soil conditions arose between
395 hydrological regimes, i.e. between active and abandoned channels. While thaw front depth,
396 depth of each soil horizon, and soil bulk density were similar between hydrological regimes,
397 soils along active channels exhibited significantly 6% higher pH and 30% lower total water
398 content than those sampled along abandoned channels (Table 1, Supplementary material 5).
399 Active and abandoned channels also differed significantly in soil temperature ($P = 0.001$ and
400 $P = 0.02$ for FDD and TDD, respectively; Table 1), with abandoned channels showing 26%
401 higher FDD and 44% lower TDD than active channels (Supplementary material 5). No
402 difference in soil C:N ratio and soil total N content emerged between channel zones ($P = 0.15$
403 and $P = 0.64$, respectively; Table 1).

404 Patches of *S. richardsonii* along active and abandoned channels were not associated with
405 changes in thaw front depth and soil bulk density compared to plots dominated by prostrate
406 shrubs and graminoids (non-significant vegetation effect, $P > 0.19$ in both cases; Table 1). Soil
407 total water content and pH measured beneath *S. richardsonii* averaged 3.9% and 7.4,
408 respectively, i.e. within the range of values measured in plots outside *S. richardsonii* patches
409 ($P > 0.43$ in both cases; Supplementary material 5). Patches of *S. richardsonii* were not

410 associated either with variation in soil freezing and thawing degrees-days measured across two
411 seasons ($P > 0.26$ in both cases), which respectively averaged 5700°C and 240°C in both
412 vegetation conditions (Table 1, Supplementary material 5). There was no difference in soil C:N
413 ratio and soil total N content between vegetation conditions ($P = 0.33$ and $P = 0.28$,
414 respectively; Table 1). Yet, along active channels soil total N content increased by 37% beneath
415 *S. richardsonii* compared to plots dominated by prostrate shrubs and graminoids ($P = 0.05$).

416 **Variation in total soil organic carbon stocks**

417 Total soil organic carbon stocks (SOC_{tot}) averaged 18.0 ± 0.6 kgC m^{-3} (equivalent to 1.4 ± 0.1
418 kgC m^{-2}) across all plots (volumetric SOC data are presented in the main text; see
419 Supplementary materials 1 and 6 for surfacic SOC data). There was no significant difference
420 in SOC_{tot} between hydrological regimes, nor between vegetation conditions. While no
421 difference in SOC_{tot} arose between vegetation conditions located along abandoned channels (P
422 > 0.60), SOC_{tot} differed between vegetation conditions along active channels, with a 18-28%
423 increase in organic C in soils sampled beneath *S. richardsonii* compared to those sampled
424 outside the species' patches ($r^2 = 0.15$ and $P = 0.08$ for volumetric content, $r^2 = 0.46$ and $P =$
425 0.02 for surfacic content; Figure 3a, Supplementary material 6).

426 **Drivers of soil organic carbon stocks**

427 The model selection indicated that LAI_w and TLN_w were the variables that best represented the
428 influence of plant C supply and N demand on SOC_{tot} variation, respectively (Figure 4a). The
429 path analysis revealed that SOC_{tot} was related positively to LAI_w and negatively to TLN_w ($\rho =$
430 0.86, $P < 0.01$ and $\rho = -0.64$, $P < 0.05$, respectively; Figure 4b,c), and that together these
431 relations increased the amount of SOC_{tot} variation explained ($r^2 = 0.47$; Table 2, Figure 4d),
432 when compared with the categorical model ($r^2 = 0.15$, see earlier paragraph). The path analysis
433 also retained the covariation between LAI_w and TLN_w ($P = 0.054$), the positive effect of *S.*

richardsonii occurrence on LAI_w and TLN_w (ρ = 0.79, $P < 0.001$, and ρ = 0.55, $P < 0.01$, respectively), as well as the positive effect of hydrological regime on LAI_w and TLN_w, although the latter two relations were not significant (ρ = 0.12 and ρ = 0.40, respectively; Figure 4d). In contrast, the path analysis did not retain the direct effects of hydrological regime and *S. richardsonii* occurrence on SOC_{tot}, indicating that there was no residual effect of vegetation and environmental changes on total soil organic carbon stock.

Variation in soil organic carbon stocks across soil horizons and OM compartments

A significant difference in soil organic carbon stocks was observed between soil horizons, with stocks being consistently higher in the top soil horizon A_1 than in the soil horizon A_2 (30.0 vs 15.2 kgC m^{-3}, respectively; $P < 0.001$; Table 1, Figure 3b). There was no difference in SOC-A_1 and SOC-A_2 between hydrological regimes ($P > 0.40$ in both cases), nor between vegetation conditions (Table 1). SOC contained in horizons A_1 and A_2 did not differ between vegetation conditions along abandoned channels (P = 0.27 in the two cases; Table 1, Figure 3b). Yet, differences arose between vegetation conditions along active channels, with SOC-A_1 beneath *S. richardsonii* decreasing significantly by 21% compared to plots located outside the species' patches (27.3 vs 34.6 kgC m^{-3}; P = 0.04; Table 1, Figure 3b). SOC-A_2 also showed a 25% increase beneath *S. richardsonii* (16.7 vs 12.4 kgC m^{-3}), but the difference between vegetation conditions was not statistically significant (P = 0.14; Table 1, Figure 3b).

Analyses of SOC per OM compartment showed that soil organic carbon was consistently higher in OM compartments beneath *S. richardsonii*, the difference between vegetation conditions being particularly marked for mPOM and fPOM compartments (Table 1, Supplementary material 1). This pattern was driven by significant differences in C-mPOM and C-fPOM of the soil horizon A_2 along active channels, where both C-mPOM and C-fPOM were > 85% higher beneath than outside *S. richardsonii* patches (P = 0.03 in both cases; Table 1, Figure 3c). Contrastingly, no significant difference between vegetation conditions was found

in C-cPOM regardless of the hydrological regime and soil horizon, nor in C-mPOM and C-fPOM along abandoned channels ($P > 0.21$ in all cases; Figure 3c). The C content of the mineral-associated OM (MAOM) did not exhibit overall differences between vegetation conditions and channels ($P > 0.12$ in all cases). Yet, C-MAOM of the soil horizon A_1 was lower beneath *S. richardsonii* along active channels ($P = 0.05$; Figure 3c).

Quality of soil organic carbon

Across all plots, the increase in soil organic carbon associated with greater plant carbon supply was characterized by a change in the OM ^{13}C and ^{14}C isotopic signature. Soil bulk $\delta^{13}C$ was strongly and negatively associated with LAI_w ($r^2 = 0.58$, $P < 0.001$; Figure 5a). This effect was particularly noticeable in the horizon A_1 compared to A_2 ($r^2 = 0.50$, $P < 0.001$ and $r^2 = 0.33$, $P = 0.001$ for A_1 and A_2, respectively; Figure 5b), and in each OM compartment ($r^2 > 0.35$ and $P < 0.001$ in the three cases; Figure 5c). The lowest soil $\delta^{13}C$ values were found under high net carbon supply conditions, i.e. in plots sampled beneath *S. richardsonii* regardless of the hydrological regime, and were closer to leaf $\delta^{13}C$ signature compared to $\delta^{13}C$ of soils sampled outside *S. richardsonii* patches (Table 1, Supplementary material 7). Variation in SOM isotopes with vegetation change was also captured when analyzing OM $\mathbf{\Delta}^{14}C$ values of soil horizon A_2. Values of $\mathbf{\Delta}^{14}C$, which were lower in active than in abandoned channels for each POM compartment considered, were always higher (i.e. less negative) in plots beneath *S. richardsonii* than in plots dominated by herbaceous and other *Salix* spp. (Figure 6). The difference in $\mathbf{\Delta}^{14}C$ between vegetation conditions was particularly marked when considering the A_2-fPOM compartment sampled along active channels (94.26‰). By contrast, the difference in the A_2-fPOM $\mathbf{\Delta}^{14}C$ between vegetation conditions along abandoned channels was of 14.88‰.

Plant N demand was positively but weakly related to soil bulk $\delta^{15}N$ ($r^2 = 0.13$, $P = 0.07$; Figure 5d). The same pattern was observed in the soil horizon A_2 ($r^2 = 0.11$, $P = 0.09$; Figure 5e) and in the A_2-cPOM compartment ($r^2 = 0.09$, $P = 0.15$; Figure 5f). Soil $\delta^{15}N$ values were

484 generally less negative than the leaf $\delta^{15}N$ signature (Table 1, Supplementary material 7). The
485 highest (i.e. less negative) soil $\delta^{15}N$ values were found under high nutrient demand, i.e. in plots
486 beneath *S. richardsonii* regardless of the hydrological regime (Figure 5d).

487 Discussion

488 This study aimed at exploring how tundra shrubification and environmental changes affect soil
489 organic carbon stock dynamics in the High Arctic. We used the occurrence of *Salix richardsonii*
490 patches along channels differing in water and nutrient availability to investigate the extent to
491 which changes in soil organic carbon stocks were associated with a shift in plant economic
492 strategies. Our observational approach suggested that increasing plant productivity associated
493 with greater erect shrub abundance can lead to an increase in soil organic carbon stock
494 compared to adjacent plant communities dominated by prostrate shrubs and graminoids.
495 However, the greater soil organic carbon stocks beneath *S. richardsonii* patches were not linked
496 to direct effects of plant taxa composition or environmental changes (relations 1 and 9 in Figure
497 1), but rather to variation in plant aboveground functional traits associated with greater carbon
498 supply and nutrient demand (relations 2 and 3 in Figure 1).

499 ***S. richardsonii* increased total soil organic carbon stocks along active channels of alluvial**
500 **fans**

501 We found that total soil organic carbon stocks beneath *S. richardsonii* patches ranged from 1.05
502 to 2.00 kg m^{-2} (14.76 to 22.68 kg m^{-3}). Conducted at a latitude of 73°N in comparison with the
503 62°-68°N latitudinal range of previous work (e.g. Wilmking and others 2006; Hartley and
504 others 2012; Sørensen and others 2018; Street and others 2018; Parker and others 2021), this
505 study represents so far the northernmost evaluation of soil organic carbon stocks in the context
506 of increasing erect deciduous shrub abundance in tundra ecosystems. The stocks we found are
507 within the range of soil organic carbon pools that have been reported to date in the handful of

other erect shrub-dominated tundra sites, going from 0.93 kg m^{-2} under *Salix glauca* L. and *Salix lapponum* L. in Dovre Mountain alpine tundra, Norway (Sørensen and others 2018) and 1.66-2.79 kg m^{-2} under *Betula nana* L. and *Salix pulchra* Cham. in low Arctic tundra near Toolik Lake, AK, USA (DeMarco and others 2011; Lynch and others 2018) to 3.00 ± 0.50 kg m^{-2} under *Betula nana* L. and *Salix* spp. thickets in low Arctic tundra near Abisko, Sweden (Parker and others 2015; Parker and others 2020), 3.64 ± 1.40 kg m^{-2} under *Alnus viridis* (Chaix) DC. in low Arctic tundra near Inuvik, NWT, Canada (Street and others 2018) and 6.00 kg m^{-2} under *Betula glandulosa* Michx. in subarctic tundra near Umiujaq, QC, Canada (Gagnon and others 2019).

Our observations underscore the potential of *S. richardsonii* to increase soil organic carbon stocks compared to neighboring prostrate tundra when local environmental conditions are suitable. This plant-environment interaction observed from a fine-scale paired sampling is particularly striking considering that changes in soil organic carbon stocks are usually difficult to detect due to their large pool size, slow turnover rate and substantial spatial heterogeneity (van Groenigen and others 2014). As *S. richardsonii* in the studied sites are probably older than 100 years (Bisson 2016), further analyses are now required using root collars, which might be buried deep considering the sedimentation process occurring in this system, to determine the period of time over which such shrub-mediated increase in soil organic carbon stocks has occurred. In addition, a recent evaluation of soil carbon stocks of dominant geomorphological terrain units conducted in the same valley as our study sites showed that alluvial fans can store up to 25 kgC m^{-3} within the first 5 cm of soil (Ola and others 2022), which is in the same order of magnitude as the SOC values we found. It now remains to be seen how variation in catchment size, channel slope, run off, and sedimentation rates among alluvial fans of the valley influence these findings.

532 The increase in soil organic carbon stocks beneath *S. richardsonii* along active channels of
533 alluvial fans differs from the majority of carbon cycle studies that were carried out among low
534 arctic and subarctic tundra ecotones, and that reported either no change (Lynch and others 2018)
535 or a depletion in soil organic carbon pools in erect shrub sites compared to adjacent heath and
536 meadow systems (e.g. Wilmking and others 2006; Hartley and others 2012; Sørensen and
537 others 2018). The discrepancy among studies may be in part explained by the fact that they
538 primarily linked soil carbon storage to changes in plant community composition, regardless of
539 the functional mechanisms of soil carbon stock variation. This is also illustrated by the results
540 of Kemppinen and others (2021), who found that soil organic carbon stocks were positively
541 related to overall plant coverage and woody plant height, and negatively to woody plant
542 dominance. Accounting only for changes in plant taxa composition or plant functional groups
543 might thus limit our mechanistic understanding of the effects of increasing erect shrub
544 abundance on soil carbon storage. Alternatively, we found that the magnitude of variation in
545 soil organic carbon stocks can be affected by the depth of soil horizons considered. While most
546 studies have to date reported soil carbon stocks per unit surface (Parker and others 2021), also
547 providing estimates of soil carbon stocks per unit volume might further inform about how
548 organic carbon is distributed along soil profiles.

549 **Biological drivers of soil organic carbon stock variation**

550 Soil conditions such as total water content, thermal status and thaw front depth were similar
551 beneath and outside *S. richardsonii* patches, and are thus unlikely to explain the contrasting
552 soil organic carbon stocks between vegetation conditions (relation 1 in Figure 1). In the active
553 channel zones characterized by regular water flows and nutrient inputs, the higher carbon stocks
554 beneath *S. richardsonii* may rather be a consequence of the response of plant resource
555 acquisition traits to favorable growing conditions. Indeed, *S. richardsonii* exhibited higher LAI
556 and greater leaf and stem biomass compared to adjacent vegetation dominated by prostrate

557 *Salix arctica* and *S. reticulata*, leading to higher plant carbon supply that outweighed potential
558 carbon losses from soil respiration (relation 5 in Figure 1). Comparatively, the increase in soil
559 organic carbon stocks beneath *S. richardsonii* patches did not hold true in the abandoned
560 channel zones. In these habitats with more limited water flows and nutrient inputs, the reduction
561 in LAI compared to active channel zones may be responsible for the lack of influence of *S.*
562 *richardsonii* dominance on soil organic carbon stocks. Such trait variation along abiotic
563 gradients supports observations throughout the tundra that plant trait attributes strongly respond
564 to local variability in environmental conditions (Bret-Harte and others 2001; Bjorkman and
565 others 2018).

566 Irrespective of channel zones and vegetation conditions, soil organic carbon decreased for a
567 given LAI with increasing TLN (relation 3 in Figure 1). This suggests that increasing nutrient
568 demand has likely led to a N-limiting situation, which has stimulated plant-enhanced
569 mineralization, in turn inducing a decrease in SOC. In line with all other studies showing that
570 tundra is particularly limited by nutrients (Chapin and others 1995; Elser and others 2007;
571 Keuper et al. 2020), our result highlighted the importance of considering plant nutrient demand
572 when quantifying the influence of vegetation changes and plant-enhanced mineralization on
573 soil carbon content. They support observations by Henneron and others (2020b), who found
574 that differences in soil organic carbon mineralization among temperate grassland species were
575 related to interspecific variation in economic strategies that sustain nutrition. Specifically, soil
576 under fast-growing species with higher photosynthetic rates and greater aboveground biomass
577 exhibited higher carbon mineralization than soil under slow-growing conservative species
578 (Henneron and others 2020b). While photosynthetic rates have yet to be measured at our study
579 sites, we still found that soil carbon content beneath *S. richardsonii* was associated with high
580 leaf biomass and related high total nutrient demand. This further indicates that biomass-related
581 traits such as LAI are key features to consider when studying how plant nutrition controls soil

582 C dynamics, in addition to the traits captured within the leaf economics spectrum (LES;
583 Henneron and others 2020a; Terrer and others 2021). For instance, leaf N content, which
584 belongs to the LES, does not necessarily correlate with plant N demand, which belongs to the
585 plant height-biomass spectrum (Maire and others 2009).

586 According to our assumption, we showed that a functional trait-based approach is beneficial
587 to provide new insights into how vegetation changes regulate tundra carbon cycling. Through
588 the path analysis, we showed that only traits were required to explain SOC variation in the
589 studied system, whereas all the other vegetation conditions such as moss and root biomass were
590 not. Our study agrees with the findings of Happonen and others (2022), who showed that
591 aboveground plant traits had strong relationships with either aboveground or soil carbon stocks.
592 It also highlights the relevance of using LAI to characterize vegetation effects on carbon cycling
593 in the tundra (Shaver and others 2007; Street and others 2007; Parker and others 2020). The
594 fact that in the study of Happonen and others (2022) soil carbon stocks were significantly
595 related to SLA and LDMC instead of plant height further suggests that measuring leaf economic
596 traits, that integrate plant investment in carbon and nutrients (Wright and others 2004), are key
597 for a better mechanistic understanding of vegetation-carbon interactions. The strong and
598 negative relationship between soil organic carbon stocks and TLN demonstrates that
599 considering functional traits related to plant nutrient demand in parallel of those associated with
600 carbon supply is important to better characterize plant-soil linkages that shape the fate of soil
601 carbon stocks in tundra landscapes.

602 The explanatory power of our models was relatively high even if we only considered a few
603 plant aboveground traits as proxies of carbon supply and nutrient demand dynamics.
604 Particularly, all the other vegetation conditions not associated with traits were not required in
605 our path analysis model (relation 1 in Figure 1). Yet, vegetation changes also induce significant
606 shifts in plant-mycorrhizal associations and microbial community (Deslippe and others 2011;

607 Clemmensen and others 2021). Shifts in soil carbon storage between vegetation conditions are
608 likely to be also driven by rhizosphere microbiome and fine rooting traits involved in plant-soil
609 feedbacks (Parker and others 2021; Spitzer and others 2022). Further attention on belowground
610 processes will thus be required, especially in sites where increasing erect shrub abundance is
611 associated with changes in woody plant taxa.

612 **Regulation of soil isotopic signatures**

613 Differences between vegetation conditions in soil stable $\delta^{13}C$ and $\delta^{15}N$ and radioactive ^{14}C
614 isotopes illustrated that *S. richardsonii* has strongly influenced soil chemistry and stability of
615 SOM stocks, in accordance with the well documented effects of plant economic traits on soil
616 biogeochemistry (Zhu and others 2016; Henneron and others 2020a). These results also align
617 with changes in soil carbon supply and nutrient demand dynamics. Greater LAI_w (i.e. greater
618 carbon supply) was associated with more negative $\delta^{13}C$ in all soil horizons and OM
619 compartments (Supplementary material 7), suggesting that new plant-derived carbon, depleted
620 in ^{13}C because of the Suess effect (Ehleringer and others 2000), has been incorporated into all
621 soil compartments (Figure 5, Supplementary material 7). The steeper slope of the $\delta^{13}C$-LAI_w
622 relationship for the top soil horizon A_1 compared to the soil horizon A_2 (Figure 5b) indicates
623 that the input of new carbon may be greater in the first two centimeters of soils, where we found
624 the vast majority of roots. However, the amount of new carbon in the soil horizon A_2 along
625 active channels was significant enough to increase soil organic carbon stocks and rejuvenate
626 the $\mathbf{\Delta}^{14}C$ signature of the fPOM compartment from -291‰ to -197‰ (Figure 6), which is
627 equivalent to a mean age shift from 2809 ± 86 to 1619 ± 80 years (based on Crann and others
628 2017). We also observed a higher elevation of the $\delta^{13}C$-LAI_w relationship for the fPOM
629 compartment (Figure 5c). It is likely that the fPOM compartment incorporated minerals
630 associated with less-depleted carbon compounds such as carbohydrate, sugar, proteins and

631 microbial product (Lavallee and others 2020), whereas cPOM and mPOM compartments were
632 mostly constituted by highly-depleted lignin (Camino-Serrano and others 2019).

633 Finally, the lower SOC-A_1 beneath *S. richardsonii*, in conjunction with the higher soil bulk
634 $\delta^{15}N$ with greater TLN_w in the soil horizon A_2 (Figure 5e), suggests that rhizosphere priming
635 might also contribute to the soil organic carbon dynamics in our sites. The increase in OM
636 mineralization and related positive priming have been observed in many places across the
637 Arctic (Hartley and others 2012; Keuper and others 2020). However, we did not quantify
638 priming *per se*, and therefore additional field studies are now required to ascertain the link
639 between plant nutrient demand traits and priming-driven soil carbon loss. In addition, analyses
640 of carbon isotopes can involve potential sources of error, and we are aware that this study has
641 some limitations that should be considered when placing the results in the geomorphological
642 context of the valley. The studied sites are located along alluvial fans that allow for running
643 water and deposition of sediments and carbon coming from the bordering plateau (Fortier and
644 others 2006). Additional ^{14}C measurements across additional fluxes and pools would fine-tune
645 the temporal dynamics of active and abandoned channels, and consequently that of *S.*
646 *richardsonii* colonization.

647 **Conclusion**

648 Structural changes related to greater erect shrub abundance in the Arctic are strong regulators
649 of soil organic carbon stocks through optimization of aboveground functional traits associated
650 with carbon and nutrient acquisition dynamics. This study first highlights that the use of plant
651 economic strategies instead of vegetation composition or plant functional groups may provide
652 new insights on carbon cycling variation with vegetation changes. It remains to be tested to
653 what extent other plant compartments such as roots and leaf litter contribute to differences in
654 soil organic carbon stocks between vegetation conditions. Moreover, we evaluated soil organic
655 carbon stocks along alluvial fans specifically, and complement in that way the handful of

studies that so far have provided soil carbon contents by accounting for the specificity of geomorphological terrain units in the Arctic. Lastly, fine-scale plant-environment interactions suggest that estimating soil organic carbon stocks locally may be difficult to extrapolate over larger areas, illustrating the need for carbon cycle studies in many more sites across the Arctic. In that context, establishing common functional trait-based methodologies that are easily applicable globally has the potential to foster our understanding of the consequences of vegetation changes on Arctic ecosystem carbon storage.

Acknowledgements

The authors are thankful to the Inuit community of Pond Inlet and to Parks Canada-Sirmilik National Park, and grateful to Ariane Bisson for her fieldwork support and to Annie Picard, Joannie Vertefeuille and Hugo Tremblay for their help with soil core processing and preliminary data analyses. This study was supported by the Fonds de Recherche du Québec—Nature et technologies (FRQNT-2018-PR-208107), the Natural Sciences and Engineering Research Council of Canada (NSERC) Discovery Frontiers grant 'Arctic Development and Adaptation to Permafrost in Transition' (ADAPT), the Network of Centers of Excellence of Canada ArcticNet, the Northern Scientific Training Program (Indian and Northern Affairs Canada), the Laval University and the University of Québec at Trois-Rivières. L.J.L. and M.T. were supported by EnviroNorth Interdisciplinary research fellowships (2014-2015) and the UQTR Research Chair in Functional Arctic Ecology (2019-2022). V.M., E.L. and F.G. were supported by NSERC Discovery grants. Logistical support for field work and access to the Bylot Island field camp during summers 2015-2018 were provided by the Centre d'études nordiques (CEN) and Polar Continental Shelf Program (Natural Resources Canada).

References

Acton P, Fox J, Campbell E, Rowe H, Wilkinson M. 2013. Carbon isotopes for estimating soil decomposition and physical mixing in well-drained forest soils. Journal of Geophysical Research: Biogeosciences 118: 1532–1545.
Bates D, Mächler M, Bolker B, Walker S. 2015. Fitting linear mixed-effects models using lme4. Journal of Statistical Software 67: 1–48.
Bisson A. 2016. Étude dendroécologique de l'arbuste érigée *Salix richardsonii* à sa limite nordique de distribution dans le Haut-Arctique. Trois-Rivières: Université du Québec à Trois-Rivières. 11p.
Bjorkman, AD, Myers-Smith IH, Elmendrof SC, Normand S, Rüger N, Beck PSA, Blach-Overgaard A, Blok D, Cornelissen JHC, Forbes BC et al. 2018. Plant functional trait change across a warming tundra biome. Nature 562: 57-62.
Blair TC, McPherson JG. 2009. Processes and forms of alluvial fans. Parsons AJ, Abrahams AD, editors. Geomorphology of Desert Environments. Dordrecht: Springer. 831p.
Bret-Harte MS, Shaver GR, Zoerner JP, Johnstone JF, Wagner JL, Chavez AS, Gunkelman IV RF, Lippert SC, Laundre JA. 2001. Developmental plasticity allows *Betula nana* to dominate tundra subjected to an altered environment. Ecology 82: 18-32.
Camino-Serrano M, Tifani M, Balesdent J, Hatté C, Peñuelas J, Cornu S, Guenet B. 2019. Including stable carbon isotopes to evaluate the dynamics of soil carbon in the land-surface model ORCHIDEE. Journal of Advances in Modeling Earth Systems 11: 3650-3669.
Chapin III FS, Shaver GR, Giblin AE, Nadelhoffer KJ, Laundre JA. 1995. Responses of Arctic tundra to experimental and observed changes in climate. Ecology 76: 694-711.
Chen L, Fang K, Wei B, Qin S, Feng X, Hu T, Ji C, Yang Y. 2021. Soil carbon persistence governed by plant input and mineral protection at regional and global scales. Ecology Letters 24: 1018-1028.
Clemmensen KE, Brandström Durling M, Michelsen A, Hallin S, Finlay RD, Lindahl BDA. 2021. tipping point in carbon storage when forest expands into tundra is related to mycorrhizal recycling of nitrogen. Ecology Letters 24: 1193-1204.
Cornelissen JHC, Van Bodegom PM, Aerts R, Callaghan TV, Van Logtestijn RSP, Alatalo J, Chapin III FS, Gerdol R, Gudmundson J, Gwynn-Jones D et al. 2007. Global negative vegetation feedback to climate warming responses of leaf litter decomposition rates in cold biomes. Ecology Letters 10: 619-627.
Coulombe S, Fortier D, Bouchard F, Paquette M, Charbonneau S, Lacelle D, Laurion I, Pienitz R. 2022. Contrasted geomorphological and limnological properties of thermokarst lakes formed in buried glacier ice and ice-wedge polygon terrain. The Cryosphere 16: 1637-1657.
Craine JM, Brookshire ENJ, Cramer MD, Hasselquist NJ, Koba K, Marin-Spiotta E, Wang L. 2015. Ecological interpretation of nitrogen isotope ratios of terrestrial plants and soils. Plant & Soil 396: 1-26.
Crann CA, Murseli S, St-Jean G, Zhao X, Clark ID, Kieser WE. 2017. First status report on radiocarbon sample preparation at the A.E. Lalonde AMS Laboratory (Ottawa, Canada). Radiocarbon 59: 695-704.
Daubenmire R. 1959. A canopy-coverage method of vegetational analysis. Northwest Science 33: 43–64.
DeMarco J, Mack MC, Bret-Harte MS. 2011. The effects of snow, soil, microenvironment, and soil organic matter quality on N availability in three Alaskan arctic plant communities. Ecosystems 14: 804-817.
DeMarco J, Mack MC, Bret-Harte MS. 2014. Effects of arctic shrub expansion on biophysical vs. biogeochemical drivers of litter decomposition. Ecology 95: 1861-1875.
Deslippe JR, Hartmann M, Mohn WW, Simard SW. 2011. Long-term experimental manipulation of climate alters the ectomyccorhizal community of *Betula nana* in Arctic tundra. Global Change Biology 17: 1625-1636.

729 Dhillion SS. 1994. Ectomycorrhizae, arbuscular mycorrhizae, and *Rhizoctonia* sp. of alpine and
730 boreal *Salix* spp. in Norway. Arctic and Alpine Research 26: 304-307.
731 Dijkstra FA. 2009. Modeling the flow of ^{15}N after a ^{15}N pulse to study long-term N dynamics
732 in a semiarid grassland. Ecology 90: 2171-2182.
733 Dijkstra FA, Bader NE, Johnson DW, Cheng W. 2009. Does accelerated soil organic matter
734 decomposition in the presence of plants increase plant N availability? Soil Biology and
735 Biochemistry 41: 1080-1087.
736 Dijkstra, FA, Carrillo Y, Pendall E, Morgan JA. 2013. Rhizosphere priming: a nutrient
737 perspective. Frontiers in Microbiology 4: 216.
738 Domine F, Barrere M, Morin S. 2016. The growth of shrubs on high Arctic tundra at Bylot
739 Island: impact on snow physical properties and permafrost thermal regime. Biogeosciences
740 13: 6471–6486.
741 Ehleringer J, Buchmann N, Flanagan LB. 2000. Carbon isotope ratios in belowground carbon
742 cycle processes. Ecological Applications 10: 412-422.
743 Ellis CJ, Rochefort L. 2004. Century-scale development of polygon-patterned tundra wetland,
744 Bylot Island (73° N, 80° W). Ecology 4: 963-978.
745 Ellis CJ, Rochefort L, Gauthier G, Pienitz R. 2008. Paleoecological evidence for transitions
746 between contrasting landforms in a polygon-patterned High Arctic wetland. Arctic,
747 Antarctic, and Alpine Research 40: 624–637.
748 Elmendorf SC, Henry GHR, Hollister RD, Björk RG, Boulanger-Lapointe N, Cooper EJ,
749 Cornelissen JHC, Day TA, Dorrepaal E, Elumeeva TG et al. 2012. Plot-scale evidence of
750 tundra vegetation change and links to recent summer warming. Nature Climate Change 2:
751 453-457.
752 Elser JJ, Bracken MES, Cleland ES, Gruner DS, Harpole WS, Hillebrand H, Ngai JT, Seabloom
753 EW, Shurin JB, Smith JE. 2007. Global analysis of nitrogen and phosphorus limitation of
754 primary producers in freshwater, marine and terrestrial ecosystems. Ecology Letters 10:
755 1135-1142.
756 Epstein HE, Myers-Smith I, Walker DA. 2013. Recent dynamics of arctic and sub-arctic
757 vegetation. Environmental Research Letters 8: 015040.
758 Fontaine S, Barot S. 2005. Size and functional diversity of microbe populations control plant
759 persistence and long-term soil carbon accumulation. Ecology Letters 8: 1075-1087.
760 Fontaine S, Bardoux G, Abbadie L, Mariotti A. 2004. Carbon input to soil may decrease soil
761 carbon content. Ecology Letters 7: 314-320.
762 Fontaine S, Henault C, Aamor A, Bdioui N, Bloor JMG, Maire V, Mary B, Revaillot S, Maron
763 PA. 2011. Fungi mediate long term sequestration of carbon and nitrogen in soil through their
764 priming effect. Soil Biology & Biochemistry 43: 86-96.
765 Fortier D, Allard M. 2004. Late Holocene syngenetic ice-wedge polygons development, Bylot
766 Island, Canadian Arctic Archipelago. Canadian Journal of Earth Science 41: 997–1012.
767 Fortier D, Allard M, Pivot F. 2006. A late-Holocene record of loess deposition in ice-wedge
768 polygons reflecting wind activity and ground moisture conditions, Bylot Island, eastern
769 Canadian Arctic. The Holocene 16: 635-646.
770 Gagnon M, Domine F, Boudreau S. 2019. The carbon sink due to shrub growth on Arctic
771 tundra: a case study in a carbon-poor in eastern Canada. Environmental Research
772 Communications 1: 091001.
773 Gauthier G, Bêty J, Cadieux M-C, Legagneux P, Doiron M, Chevallier C, Lai S, Tarroux A,
774 Berteaux D. 2013. Long-term monitoring at multiple trophic levels suggest heterogeneity in
775 responses to climate change in the Canadian Arctic tundra. Philosophical Transactions of
776 the Royal Society B 368: 20120842.
777 Gavazov K, Canarini A, Jassey VEJ, Mills R, Richter A, Sundqvist MK, Väisänen M, Walker
778 TWN, Wardle DA, Dorrepaal E. 2022. Plant-microbial linkages underpin carbon

sequestration in contrasting mountain tundra vegetation types. Soil Biology and Biochemistry 165: 108530.
Givnish TJ, Wong SC, Stuart-Williams H, Holloway-Phillips M, Farquhar GD. 2014. Determinants of maximum tree height in *Eucalyptus* species along a rainfall gradient in Victoria, Australia. Ecology 95: 2991-3007.
Gu Q, Grogan, P. 2020. Responses of low Arctic tundra plants species to experimental manipulations: Differences between abiotic and biotic factors and between short- and long-term effects. Arctic, Antarctic, and Alpine Research 52: 524-540.
Happonen K, Virkkala A-M, Kemppinen J, Niittynen P, Luoto M. 2022. Relationships between above-ground plant traits and carbon cycling in tundra plant communities. Journal of Ecology 110: 700-716.
Hartley IP, Garnett MH, Sommerkorn M, Hopkins DW, Fletcher BJ, Sloan VL, Phoenix GK, Wookey PA. 2012. A potential loss of carbon associated with greater plant growth in the European Arctic. Nature Climate Change 2: 875-879.
Henneron L, Cros C, Picon-Cochard C, Rahimian V, Fontaine S. 2020a. Plant economic strategies of grassland species control soil carbon dynamics through rhizodeposition. Journal of Ecology 108: 528-545.
Henneron L, Kardol P, Wardle D, Cros C, Fontaine S. 2020b. Rhizospere control of soil nitrogen cycling: a key component of plant economic strategies. New Phytologist 228: 1269-1282.
Hobbie JE, Hobbie EA. 2009. ^{15}N in symbiotic fungi and plants estimates nitrogen and carbon flux rates in Arctic tundra. Ecology 87: 816-822.
Huo C, Luo Y, Cheng W. 2017. Rhizosphere priming effect: A meta-analysis. Soil Biology and Biochemistry 111: 78-84.
Juszak I, Eugster W, Heijmans MMPD, Schaepman-Strub G. 2018. Contrasting radiation and soil heat fluxes in Arctic shrub and wet sedge tundra. Biogeosciences 13: 4049-4064.
Kallenbach CM, Frey SD, Grandy AS. 2016. Direct evidence for microbial-derived soil organic matter formation and its ecophysiological controls. Nature Communications 7: 13630.
Kemppinen J, Niittynen P, Virkkala A-M, Happonen K, Riihimäki H, Aalto J, Luoto M. 2021. Dwarf shrubs impact tundra soils: drier, colder, and less organic carbon. Ecosystems 24: 1378-1392.
Keuper F, Wild B, Kummu M, Beer C, Blume-Werry G, Fontaine S, Gavazov K, Gentsch N, Guggenberger G, Hugelius G. et al. 2020. Carbon loss from northern circumpolar permafrost soils amplified by rhizosphere priming. Nature Geoscience 13: 560-565.
Kou D, Yang G, Li F, Feng X, Zhang D, Mao C, Zhang Q, Peng Y, Ji C, Zhu Q et al. 2022. Progressive nitrogen limitation across the Tibetan alpine permafrost region. Nature Communications 11: 3331.
Lavallee JM, Soong JL, Cotrufo MF. 2020. Conceptualizing soil organic matter into particulate and mineral-associated forms to address global change in the 21st century. Global Change Biology 26: 261-273.
Lefcheck JS. 2016. piecewiseSEM: Piecewise structural equation modelling in R for ecology, evolution, and systematics. Methods in Ecology and Evolution 7: 573-579.
Legagneux P, Gauthier G, Berteaux D, Bêty J, Cadieux M-C, Bilodeau F, Bolduc E, McKinnon L, Tarroux A, Therrien J-F, Morissette L, Krebs CJ. 2012. Disentangling trophic relationships in a High Arctic tundra ecosystem through food web modeling. Ecology 93: 1707-1716.
Liang J, Zhou Z, Huo C, Shi Z, Cole JR, Huang L, Konstantinidis KT, Li X, Liu B, Luo Z et al. 2018. More replenishment than priming loss of soil organic carbon with additional carbon input. Nature Communications 9: 3175.

Lonne I, Nemec W. 2004. High-Arctic fan delta recording deglaciation and environment disequilibrium. Sedimentology 51: 553-589.
Loya WM, Johnson LC, Kling GW, King JY, Reeburgh WS, Nadelhoffer KJ. 2002. Pulse-labeling studies of carbon cycling in arctic tundra ecosystems: Contribution of photosynthates to soil organic matter. Global Biogeochemical Cycles 16: 1-8.
Lynch LM, Machmuller MB, Cotrufo MF, Paul EA, Wallestein MD. 2018. Tracking the fate of fresh carbon in the Arctic tundra: Will shrub expansion alter responses of soil organic matter to warming? Soil Biology and Biochemistry 120: 134-144.
Maire V, Gross N, Hill D, Martin R, Wirth C, Wright IJ, Soussana F. 2013. Disentangling coordination among functional traits using an individual-centered model: impact on plant performance at intra- and inter-specific levels. PLoS ONE 8: e77372.
Maire V, Gross N, da Silveira Pontes L, Picon-Cochard C, Soussana J-F. 2009. Trade-off between root nitrogen acquisition and shoot nitrogen utilization across 13 co-occurring pasture grass species. Functional Ecology 23: 668-679.
Marsh P, Bartlett P, MacKay M, Pohl S, Lantz T. 2010. Snowmelt energetics at a shrub tundra site in the western Canadian Arctic. Hydrological Processes 24: 3603-3620.
Martel YA, Paul EA. 1974. Effects of cultivation of the organic matter of grassland soils as determined by fractionation and radiocarbon dating. Canadian Journal of Soil Science 54: 419-426.
McFadden JP, Chapin III FS, Hollinger DY. 1998. Subgrid-scale variability in the surface energy balance of arctic tundra. Journal of Geophysical Research 103: 28,947-28,961.
Mekonnen, ZA, Riley WJ, Grant RF. 2018. 21st century tundra shrubification could enhance net carbon uptake of North America Arctic tundra under an RCP8.5 climate trajectory. Environment Research Letter 13: 54029.
Metcalfe DB, Hermans TDG, Ahlstrand J, Becker M, Berggren M, Björk RG, Björkman MP, Blok D, Chaudhary N, Chisholm C et al. 2018. Patchy field sampling biases understanding of climate change impacts across the Arctic. Nature Ecology & Evolution 2: 1443-1448.
Miall ÀD, Balkwill HR, Hopkins WS Jr. 1980. Cretaceous and tertiary sediments of eclipse trough, Bylot Island area, Arctic Canada, and their regional setting. Geological Survey of Canada, paper 79-23, 20p.
Myers-Smith IH, Hik DS. 2013. Shrub canopies influence soil temperatures but not nutrient dynamics: An experimental test of tundra snow-shrub interactions. Ecology and Evolution 3: 3683-3700.
Myers-Smith IH, Elmendorf SC, Beck PSA, Wilmking M, Hallinger M, Blok D, Tape KD, Rayback SA, Macias-Fauria M, Forbes BC et al. 2015. Climate sensitivity of shrub growth across the tundra biome. Nature Climate Change 5: 887-891.
Myers-Smith IH, Forbes BC, Wilmking M, Hallinger M, Lantz T, Blok D, Tape KD, Macias-Fauria M, Sass-Klaassen U, Lévesque E et al. 2011. Shrub expansion in tundra ecosystems: dynamics, impacts and research priorities. Environmental Research Letters 6: 045509.
Myers-Smith IH, Kerby JT, Phoenix GK, Bjerke JW, Epstein HE, Assmann JJ, John C, Andreu-Hayles L, Angers-Blondin S, Beck PSA et al. 2020. Complexity revealed in the greening of the Arctic. Nature Climate Change 10: 106-117.
Ola A, Fortier D, Coulombe S, Comte J, Domine F. 2022. The distribution of soil carbon and nitrogen stocks among dominant geomorphological terrain units in Qarlikturvik Valley, Bylot Island, Arctic Canada. Journal of Geophysical Research: Biogeosciences 127: e2021JG006750.
Parker TC, Clemmensen KE, Friggens NL, Hartley IP, Johnson D, Lindahl BD, Olofsson J, Siewert MB, Street LE, Subke J-A, Wookey PA. 2020. Rhizosphere allocation by canopy-forming species dominates soil CO_2 efflux in a subarctic landscape. New Phytologist 227: 1818-1830.

878 Parker TC, Thurston AM, Raundrup K, Subke J-A, Wookey PA, Hartley IP. 2021. Shrub
879 expansion in the Arctic may induce large-scale carbon losses due to changes in plant-soil
880 interactions. Plant and Soil 463: 643-651.
881 Perreault N, Lévesque E, Fortier D, Lamarque LJ. 2016. Thermo-erosion gullies boost the
882 transition from wet to mesic tundra vegetation. Biogeosciences 13: 1237-1253.
883 Perveen N, Barot S, Alvarez G, Klumpp K, Martin R, Rapaport A, Herfurth D, Louault F,
884 Fontaine S. 2014. Priming effect and microbial diversity in ecosystem functioning and
885 response to global change: A modeling approach using the SYMPHONY model. Global
886 Change Biology 20: 1174-1190.
887 Pike N. 2011. Using false discovery rates for multiple comparisons in ecology and evolution.
888 Methods in Ecology and Evolution 2: 278-282.
889 Pouliot R, Rochefort L, Gauthier G. 2009. Moss carpets constrain the fertilizing effects of
890 herbivores on graminoid plants in arctic polygon fens. Botany 87: 1209-1222.
891 Prater I, Zubrzycki S, Buegger F, Zoor-Füllgraff LC, Angst G, Dannenmann M, Mueller CW.
892 2020. From fibrous plant residues to mineral-associated organic carbon – the fate of organic
893 matter in Arctic permafrost soils. Biogeosciences 17: 3367-3383.
894 Qian H, Joseph R, Zeng N. 2010. Enhanced terrestrial carbon uptake in the Northern High
895 Latitudes in the 21st century from the Coupled Carbon Cycle Climate Model
896 Intercomparison Project model projections. Global Change Biology 16: 641-656.
897 Rioux K. 2021. Impacts de la dégradation du pergélisol par thermo-érosion sur les processus
898 hydrologiques et les flux de matières. MSc thesis. Montréal: Université de Montréal. 98p.
899 Rousk K, Sorensen PL, Michelsen A. 2017. Nitrogen fixation in the High Arctic: a source of
900 'new' nitrogen? Biogeochemistry 136: 213–222.
901 Segal AD, Sullivan PF. 2014. Identifying the sources and uncertainties of ecosystem respiration
902 in Arctic tussock tundra. Biogeochemistry 121: 489-503.
903 Shaver GR, Rastetter EB, Salman V, Street LE, van de Weg MJ, Rocha A, van Wijk MT,
904 Williams M. 2013. Pan-Arctic modelling of net ecosystem exchange of CO_2. Philosophical
905 Transactions of the Royal Society B 368: 20120485.
906 Shaver GR, Street LE, Rastetter EB, Van Wijk MT, Williams M. 2007. Functional convergence
907 in regulation of net CO_2 flux in heterogeneous tundra landscapes in Alaska and Sweden.
908 Journal of Ecology 95: 802-817.
909 Sistla SA, Asao S, Schimel JP. 2012. Detecting microbial N-limitation in tussock tundra:
910 Implications for Arctic soil organic carbon cycling. Soil Biology & Biochemistry 55: 78-84.
911 Sistla SA, Moore JC, Simpson RT, Gough L, Shaver GR, Schimel JP. 2013. Long-term
912 warming restructures Arctic tundra without changing net soil carbon storage. Nature 497:
913 615-619.
914 Sørensen MV, Strimbeck R, Nystuen KO, Kapas RE, Enquist BJ, Graae BJ. 2018. Draining the
915 pool? Carbon storage and fluxes in three alpine plant communities. Ecosystems 21: 316-
916 330.
917 Spitzer CM, Wardle DA, Lindhal BD, Sundqvist MK, Gundale MJ, Fanin N, Kardol P. 2022.
918 Root traits and soil micro-organisms as drivers of plant-soil feedbacks within the sub-arctic
919 tundra meadow. Journal of Ecology 110: 466-478.
920 Sterck F, Markesteijn L, Schieving F, Poorter L. 2011. Functional traits determine trade-offs
921 and niches in a tropical forest community. Proceedings of the National Academy of Sciences
922 of the United States of America 108: 20627-20632.
923 Stoffel M, Conus D, Grichting MÀ, Lievre I, Maitre G. 2008. Unraveling the patterns of late
924 Holocene debris-flow activity on a cone in the Swiss Alps: chronology, environment and
925 implications for the future. Global and Planetary Change 60: 222-234.

926 Street LE, Garnett MH, Subke J-A, Baxter R, Dean JF, Wookey PA. 2020. Plant carbon
927 allocation drives turnover of old soil organic matter in permafrost tundra soils. Global
928 Change Biology 26: 4559-4571.
929 Street LE, Shaver GR, Williams M, Van Wijk MT. 2007. What is the relationship between
930 changes in canopy leaf area and changes in photosynthetic CO_2 flux in arctic ecosystems?
931 Journal of Ecology 95: 139-150.
932 Street LE, Subke J-A, Baxter R, Dinsmore KJ, Knoblauch C, Wookey PA. 2018. Ecosystem
933 carbon dynamics differ between tundra shrub types in the western Canadian Arctic.
934 Environmental Research Letters 13: 084014.
935 ter Braak CJF, Verdonschot PFM. 1995. Canonical correspondence analysis and related
936 multivariate methods in aquatic ecology. Aquatic Sciences 57: 255−289
937 Terrer C, Phillips RP, Hungate BA, Rosende J, Pett-Ridge J, Craig ME, van Groenigen KJ,
938 Keenan TF, Sulman BN, Stocker BD et al. 2021. A trade-off between plant and soil carbon
939 storage under elevated CO_2. Nature 591: 599-603.
940 Uchida M, Muraoka H, Nakatsubo T, Bekku Y, Ueno T, Kanda H, Koizumi H. 2002.
941 Photosynthesis, respiration, and production of the moss *Sanionia uncinata* on a glacier
942 foreland in the High Arctic, Ny-Ålesund, Svalbard. Arctic, Antarctic, and Alpine Research
943 34: 287-292.
944 van Groenigen KJ, Qi X, Osenberg CW, Luo Y, Hungate BA. 2014. Faster decomposition
945 under increased atmospheric CO_2 limits soil carbon storage. Science 344: 508-509.
946 Wallenstein MD, McMahon S, Schimel S. 2007. Bacterial and fungal community structure in
947 Arctic tundra tussock and shrub soils. FEMS Microbiology Ecology 59: 428-435.
948 Wilcox EJ, Keim D, de Jong T, Walker B, Sonnentag O, Sniderhan AE, Mann P, Marsch P.
949 2019. Tundra shrub expansion may amplify permafrost thaw by advancing snowmelt timing.
950 Arctic Science 5: 202-217.
951 Wilmking M, Harden J, Tape K. 2006. Effect of tree line advance on carbon storage in NW
952 Alaska. Journal of Geophysical Research-Biogeosciences 111: G02023.
953 Wright IJ, Reich PB, Westoby M, Ackerly DD, Baruch Z, Bongers F, Cavender-Bares J,
954 Chapin T, Cornelissen JHC, Flexas J et al. 2004. The worldwide leaf economics spectrum.
955 Nature 428: 821-827.
956 Zhen Z-L. 2009. Carbon and nitrogen nutrient balance signaling in plants. Plant Signaling &
957 Behaviour 4: 584-591.
958 Zhu Q, Iversen CM, Riley WJ, Slette IJ, Vander Stel HM. 2016. Root traits explain observed
959 tundra vegetation nitrogen uptake patterns: implications for trait-based land models. Journal
960 of Geophysical Research: Biogeosciences 121: 3101-3112.

Table legends

Table 1. Mean values (± 1 SE) of response variables measured in plots outside and beneath *Salix richardsonii* (*SR*) patches along active and abandoned channels. n = 6 per vegetation condition per channel, except for soil total water content (n = 12) and soil temperature (n = 3). Test statistics are for fixed effects from linear mixed models. F-values in bold indicate significant effects, which were adjusted with the FDR procedure (see Supplementary Material 2). Measurement units are as follows: biomass in gDW m^{-2} soil, LAI_w in m^2 leaf m^{-2} soil, TLN_w in g m^{-2} soil, leaf $\delta^{13}C/\delta^{15}N$ in ‰, thaw front depth in cm, soil bulk density in cm^3, soil total water content in %, soil temperature (FDD/TDD) in °C, soil total N content in kgN m^{-3} soil, and volumetric soil organic carbon stocks (SOC) in kgC m^{-3} soil.

Table 2. Results of linear mixed models testing the effect of leaf area index (LAI_w) and total leaf nutrient content (TLN_w) of woody plants (*Salix* spp.) on soil organic carbon stock. LAI_w and TLN_w were used as a proxy of plant carbon supply and nutrient demand, respectively. Predictors were scaled in the regression analysis. See Figure 4b,c for corresponding illustrations. Note that the difference between marginal and conditional r^2 corresponds to random effects (pairs of quadrats nested within channels within fans).

Table 1.

	Active channels		Abandoned channels		Channel		Vegetation		Channel x veg.	
	Outside *SR*	Beneath *SR*	Outside *SR*	Beneath *SR*	*df*	*F*	*df*	*F*	*df*	*F*
Plant traits										
Total biomass	351.0 ± 93.2	1392.2 ± 250.4	308.1 ± 70.5	1504.4 ± 281.5	1	0.03	1	**32.19**	1	0.15
Aboveground biomass	112.5 ± 46.2	1007.2 ± 199.5	252.5 ± 61.5	1416.3 ± 207.5	1	3.15	1	**51.75**	1	0.88
Root biomass	481.5 ± 181.5	780.1 ± 121.4	538.7 ± 133.4	670.5 ± 172.7	1	0.02	1	2.63	1	0.39
Shrub aboveground biomass	99.6 ± 45.6	1004.8 ± 200.0	41.1 ± 7.2	1240.2 ± 223.6	1	0.33	1	**48.57**	1	0.97
Graminoid aboveground biomass	12.9 ± 6.6	2.4 ± 1.3	3.2 ± 1.7	1.4 ± 1.2	1	1.66	1	**4.88**	1	2.41
Moss biomass	0.0 ± 0.0	0.0 ± 0.0	211.4 ± 57.4	174.7 ± 44.0	1	**28.66**	1	0.26	1	0.26
Shrub leaf biomass	35.6 ± 13.0	120.7 ± 23.1	20.7 ± 3.8	58.2 ± 25.0	1	4.14	1	**10.36**	1	1.56
Shrub stem biomass	64.0 ± 20.7	884.1 ± 185.9	17.2 ± 5.7	1182.0 ± 207.3	1	0.80	1	**50.64**	1	1.53
Leaf area index (LAI_w)	0.3 ± 0.1	1.0 ± 0.1	0.4 ± 0.1	0.7 ± 0.1	1	1.31	1	**52.89**	1	**9.51**
Total leaf nutrient content (TLN_w)	13.3 ± 5.8	51.3 ± 10.0	6.7 ± 1.7	26.3 ± 11.6	1	3.63	1	**12.17**	1	1.24
Leaf $\delta^{13}C$	-28.9 ± 0.3	-29.6 ± 0.3	-28.7 ± 0.1	-29.1 ± 0.3	1	1.90	1	2.98	1	0.18
Leaf $\delta^{15}N$	-6.7 ± 0.7	-5.5 ± 0.7	-6.1 ± 0.4	-6.0 ± 0.4	1	0.01	1	3.82	1	2.57
Soil conditions										
Thaw front depth	6.9 ± 0.1	7.6 ± 0.5	8.8 ± 0.8	8.7 ± 0.6	1	3.10	1	198.00	1	2.99
Horizon A_1 depth	1.1 ± 0.3	1.7 ± 0.4	2.2 ± 0.2	2.4 ± 0.3	1	5.70	1	3.70	1	1.03
Horizon A_2 depth	5.8 ± 0.2	5.9 ± 0.1	5.9 ± 0.2	5.6 ± 0.3	1	0.30	1	0.25	1	2.13
Soil bulk density	0.9 ± 0.1	0.8 ± 0.1	0. 8 ± 0.1	0.8 ± 0.1	1	0.43	1	0.09	1	0.07
Total water content	3.2 ± 0.3	3.1 ± 0.2	4.5 ± 0.4	4.7 ± 0.5	1	**9.10**	1	0.12	1	0.03
pH	7.6 ± 0.1	7.5 ± 0.1	7.1 ± 0.1	7.2 ± 0.1	1	**9.57**	1	0.67	1	5.16
Freezing degree-days (FDD)	5114.6 ± 220.6	4968.9 ± 114.9	6080.8 ± 174.6	6637.1 ± 428.2	1	**25.17**	1	0.61	1	1.79
Thawing degree-days (TDD)	298.0 ± 53.4	285.3 ± 67.5	223.9 ± 48.4	112.6 ± 31.3	1	**5.30**	1	1.34	1	0.85
Soil C:N ratio	9.0 ± 0.7	8.6 ± 0.3	9.0 ± 0.6	10.4 ± 0.5	1	2.36	1	1.06	1	3.23
Soil total N content	1.4 ± 0.2	2.2 ± 0.2	2.0 ± 0.2	1.7 ± 0.1	1	0.23	1	1.33	1	7.16
Soil organic carbon stocks										
Volumetric SOC_{tot}	15.62 ± 1.22	19.04 ± 1.12	18.82 ± 0.86	18.49 ± 1.03	1	1.17	1	3.09	1	4.55
Volumetric SOC-A_1	34.58 ± 4.69	27.30 ± 2.70	30.59 ± 2.15	27.37 ± 2.10	1	0.25	1	7.43	1	1.11
Volumetric SOC-A_2	12.40 ± 1.60	16.68 ± 1.87	16.24 ± 1.28	15.51 ± 0.96	1	0.65	1	1.99	1	3.98
Volumetric C-cPOM	0.73 ± 0.22	1.06 ± 0.05	1.15 ± 0.24	1.41 ± 0.31	1	2.29	1	2.43	1	0.04
Volumetric C-mPOM	0.75 ± 0.19	1.57 ± 0.31	1.38 ± 0.18	1.44 ± 0.31	1	0.85	1	3.53	1	2.71
Volumetric C-fPOM	0.61 ± 0.11	1.52 ± 0.27	1.06 ± 0.17	1.28 ± 0.26	1	0.26	1	7.26	1	2.70
Volumetric C-cPOM-A_1	3.03 ± 0.72	3.60 ± 0.76	3.08 ± 0.39	3.63 ± 0.82	1	0.00	1	0.75	1	0.00
Volumetric C-cPOM-A_2	0.40 ± 0.21	0.58 ± 0.07	0.54 ± 0.22	0.41 ± 0.07	1	0.01	1	0.03	1	1.11
Volumetric C-mPOM-A_1	5.94 ± 1.58	5.55 ± 0.58	5.51 ± 0.85	5.11 ± 1.03	1	0.14	1	0.17	1	0.00
Volumetric C-mPOM-A_2	0.05 ± 0.01	0.55 ± 0.16	0.12 ± 0.04	0.07 ± 0.01	1	6.12	1	7.49	1	10.64
Volumetric C-fPOM-A_1	4.79 ± 1.32	4.59 ± 0.48	3.91 ± 0.81	4.42 ± 0.98	1	0.26	1	0.03	1	0.17
Volumetric C-fPOM-A_2	0.08 ± 0.02	0.53 ± 0.17	0.22 ± 0.04	0.15 ± 0.02	1	1.69	1	5.45	1	9.93

Table 2.

	Soil organic carbon stock (kg C m^{-3} soil)		
	Estimate	CI	*P*
Predictors			
Intercept	18.0	(16.5, 19.5)	< 0.001
LAI_w	2.44	(1.36,3.52)	< 0.001
TLN_w	-1.79	(-2.95, -0.64)	0.002
Random effects			
σ2	3.93		
τ00 pair:(channel:fan)	0.00		
τ00 channel :fan	0.71		
τ00 fan	0.42		
Marginal r^2 / Conditional r^2			0.47 / 0.51

Figure legends

Figure 1. Conceptual model showing the direction of the expected interactions between variables in the studied system. The following paths were considered: (1) *Salix richardsonii* increases directly soil organic carbon stock, independently from plant traits. (2) Plants supply organic carbon to the soil, which increases soil organic carbon (SOC) stock. (3) Plants enhance N-rich SOC mineralization for their nutritional requirements, which not only releases mineral nutrients in the soil but also reduces SOC stock. (4) Plant C:N stoichiometry is maintained via a strong coordination between plant carbon supply and nutrient demand. The occurrence of the erect shrub *S. richardsonii* increases (5) carbon supply and (6) nutrient demand, compared to adjacent plots dominated by graminoid and prostrate shrub species. (7) Active channels provide water and nutrients to the surrounding vegetation, which stimulates plant growth and increases plant carbon supply to the soil; but they may also disturb plant standing biomass, which would decrease plant carbon supply. (8) Active channels provide water to the surrounding vegetation, which stimulates transpiration and nutrient mass-flow uptake, thus decreasing plant nutrient demand; (9) A shift in hydrological regime influence directly soil organic carbon stock, with higher organic carbon stored in soils with higher fertility, i.e. located along active channels.

Figure 2. Study location and experimental design. (a) The study was conducted in the Qarlikturvik valley of Bylot Island, Nunavut (blue circle and red rectangle in the left panel, respectively), along two alluvial fans (white rectangle in the middle panel). The white arrows in the right panel indicate the water flow going down from the plateau to the valley floor. (b) Along each fan, plant and soil materials were sampled in two hydrological regimes corresponding to active and abandoned channels (full and dotted white arrows, respectively), and where *Salix richardsonii* (*SR*) has settled. (c) In each channel zone, a paired sampling was carried out using plots where *S. richardsonii* was either present (beneath *SR*) or absent (outside

SR). Soil cores, that were on average 8 cm deep, were sampled within 0.7 m x 0.7 m quadrats. A_1 and A_2 refer to the soil horizons sampled.

Figure 3. Volumetric soil organic carbon (SOC, kg m^{-3}) outside and beneath *Salix richardsonii* (*SR*) patches located along active and abandoned channels. Horizontal lines refer to medians. Panel (a) refers to total SOC (SOC_{tot}), while panels (b) and (c) represent SOC content per horizon and OM compartment (n = 6 per vegetation condition per channel). The particulate organic matter compartments were discriminated as follows: coarse organic matter (cPOM, 2 mm to 1 mm), medium organic matter (mPOM, 1 mm to 250 µm) and fine organic matter (fPOM, 250 µm to 63 µm). The mineral-associated OM compartment (MAOM), estimated as the difference between SOC_{tot} and SOC of the three measured POM compartments, is represented for information purposes only. See Table 1 for corresponding statistics. †$P < 0.1$.

Figure 4. Influence of vegetation on total soil organic carbon stock (SOC_{tot}, kg m^{-3} soil). (a) Importance of woody plant (*Salix* spp.; c.f. subscript 'w') traits and moss biomass on SOC_{tot} variation, issued from an automated model selection analysis where the following explicative variables were considered: leaf area index (LAI_w), specific leaf area (SLA_w), total leaf nutrient (TLN_w), leaf biomass ($Leaf_w$), stem biomass ($Stem_w$), leaf nutrient content ($LNuC_w$), moss biomass, and root biomass ($Root_w$). (b,c) Conditional relationships of the mixed regression model testing the impact of (c) leaf area index (LAI_w) and (b) total leaf nutrient (TLN_w) of woody plants (*Salix* spp.) on soil organic carbon stock (i.e. volumetric SOC content; see Table 2 for model statistics). Each panel considered the effect of the variation of one explicative variable, while the second variable was considered fixed at its median value; the y-axes refer to residual values of conditional relationships. (d) Best fitted path analysis model showing the pathways that were retained from the conceptual model (Figure 1). Blue and red arrows refer to positive and negative relations, respectively. Numbers refer to the coefficients of

relationships between the predictor and response variables. Solid and dashed lines refer to significant and non-significant relations, respectively. LAI_w and TLN_w were considered as a proxy of plant net carbon supply and nutrient demand, respectively.

Figure 5. Influence of leaf area index (LAI_w) and total leaf nutrient content (TLN_w) of woody plants (*Salix* spp.) on soil organic carbon quality. LAI_w and TLN_w represent plant carbon supply and nutrient demand, respectively (see Figure 4). (a-c) Relationships between soil bulk $\delta^{13}C$ and LAI_w, determined according to (a) vegetation conditions and channel zones, (b) soil horizons, and (c) particulate OM compartments. (d-f) Relationships between soil bulk $\delta^{15}N$ and TLN_w, determined according to (d) vegetation conditions and channel zones, (e) soil horizons, and (c) particulate OM compartments of the soil horizon A_2. Relationships per OM compartments of the top soil horizon A_1 were not drawn given that no relationship was previously observed for this given horizon (see panel e).

Figure 6. Total soil organic carbon stocks (SOC_{tot}, kg m^{-3}), as quantified per vegetation condition (outside and beneath *Salix richardsonii* (*SR*) patches) and particulate organic matter compartments (cPOM, mPOM and fPOM) of soil horizon A_2, in relation to soil bulk ^{14}C (composite samples from all repetitions). The particulate organic matter compartments were discriminated as follows: coarse organic matter (cPOM, 2 mm to 1 mm), medium organic matter (mPOM, 1 mm to 250 µm) and fine organic matter (fPOM, 250 µm to 63 µm).

Figure 1

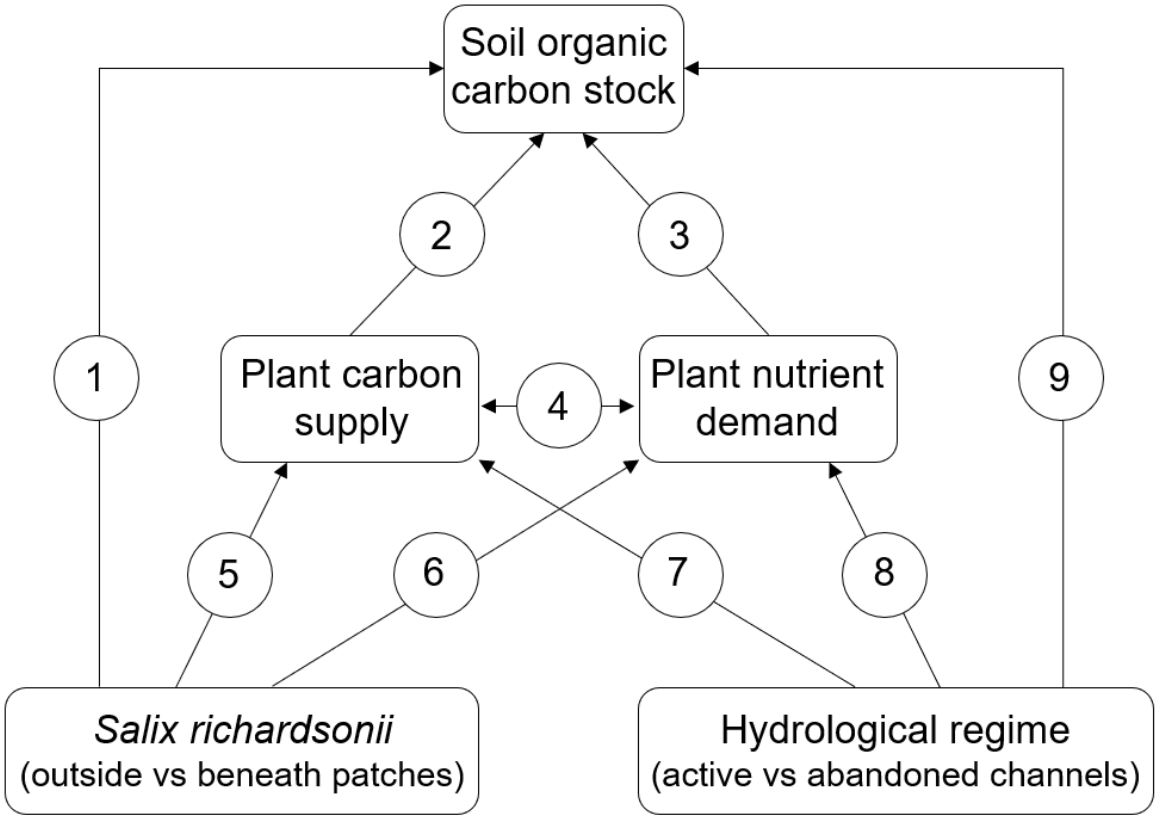
Soil organic carbon stock
2
3
1
Plant carbon supply
4
Plant nutrient demand
9
5
6
7
8
Salix richardsonii (outside vs beneath patches)
Hydrological regime (active vs abandoned channels)

Figure 2

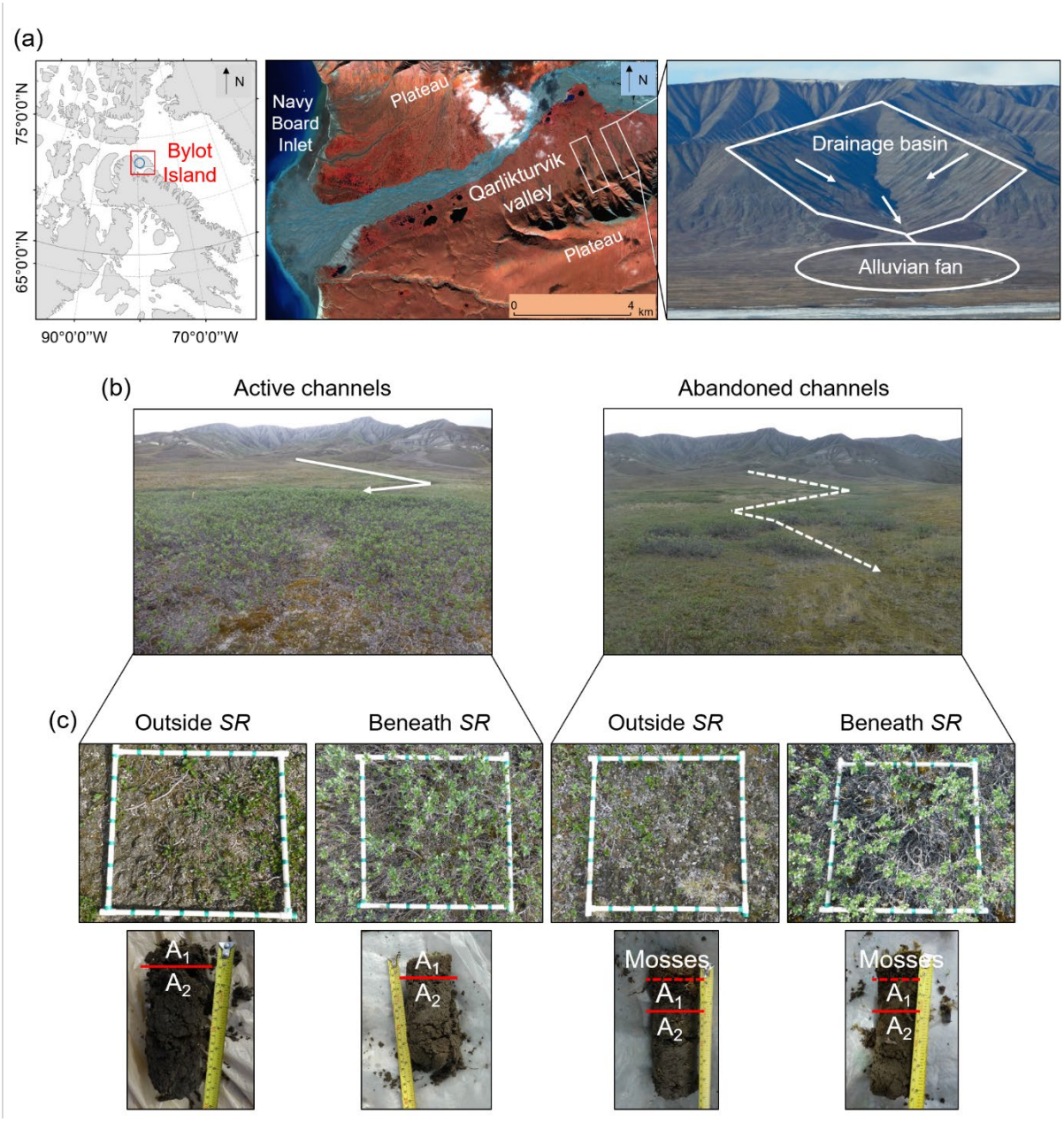
(a)
N
75°0'0"N
65°0'0"N
90°0'0"W
70°0'0"W
Bylot Island
Navy Board Inlet
Plateau
Qarlikturvik valley
Plateau
0
4 km
Drainage basin
Alluvian fan
(b)
Active channels
Abandoned channels
(c)
Outside SR
Beneath SR
Outside SR
Beneath SR
A1
A2
A1
A2
Mosses
A1
A2
Mosses
A1
A2

Figure 3

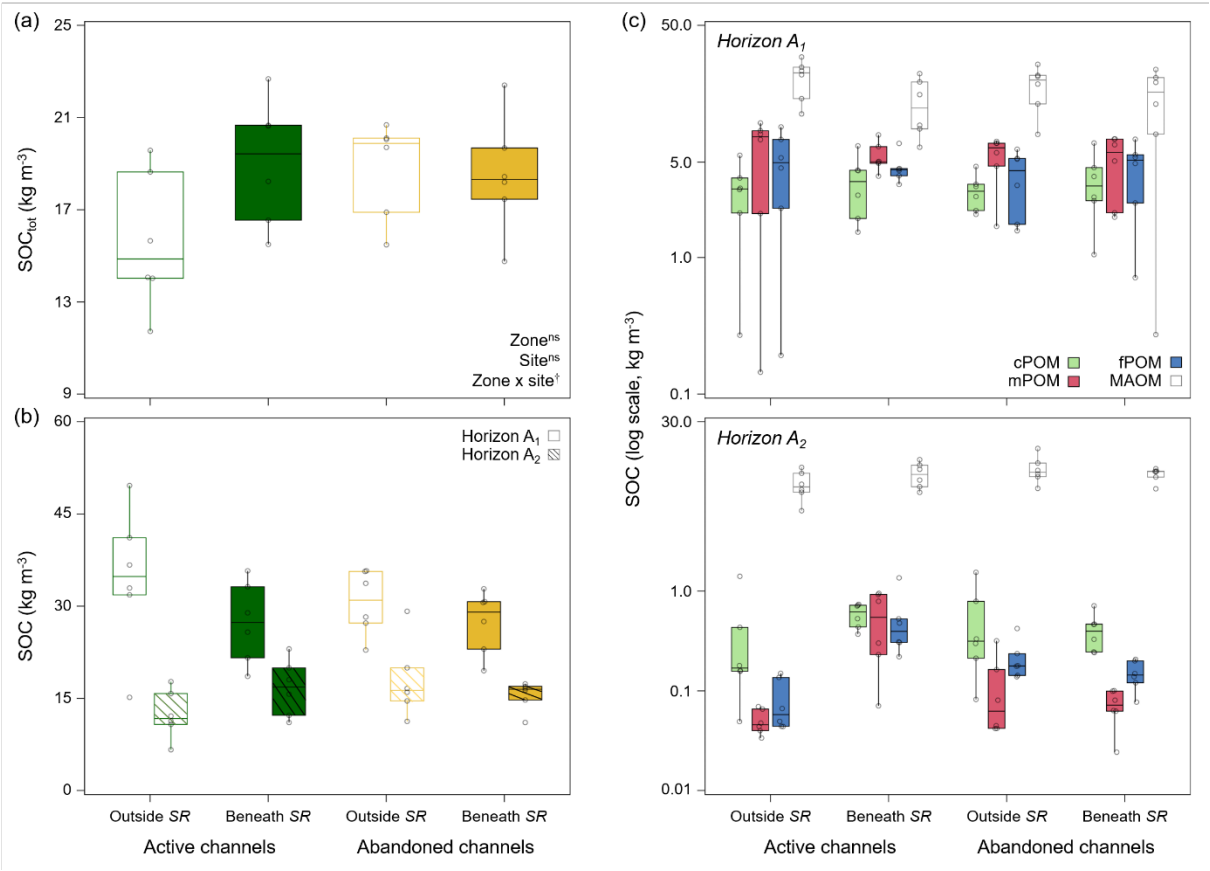
(a)
SOC$_{tot}$ (kg m^{-3})
Zone^{ns}
Site^{ns}
Zone x site†
(b)
SOC (kg m^{-3})
Horizon A$_1$
Horizon A$_2$
Outside SR
Beneath SR
Outside SR
Beneath SR
Active channels
Abandoned channels
(c)
Horizon A$_1$
Horizon A$_2$
SOC (log scale, kg m^{-3})
cPOM
mPOM
fPOM
MAOM
Outside SR
Beneath SR
Outside SR
Beneath SR
Active channels
Abandoned channels

Figure 4

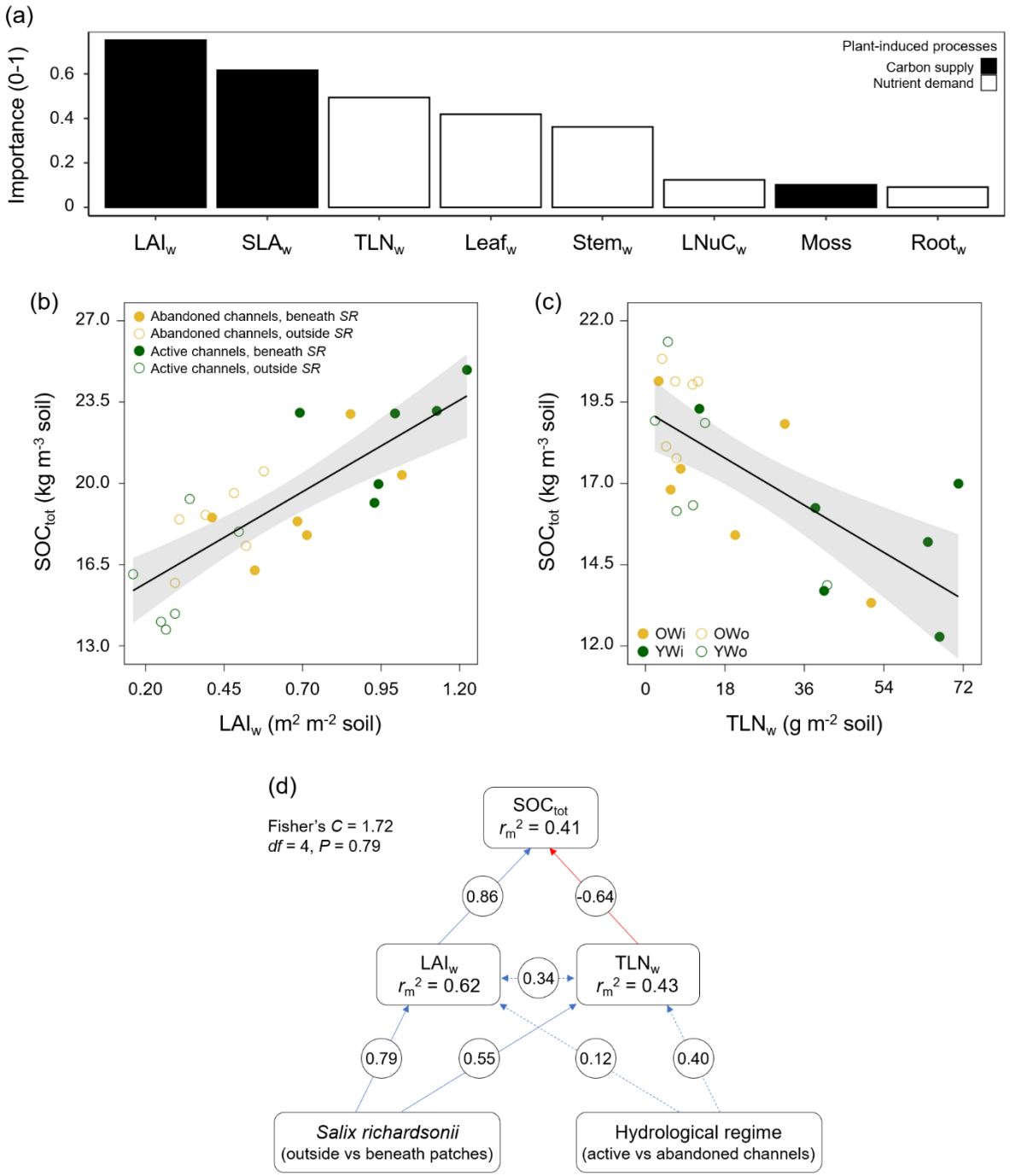
(a)
Importance (0-1)
0
0.2
0.4
0.6
Plant-induced processes
Carbon supply
Nutrient demand
LAIw
SLAw
TLNw
Leafw
Stemw
LNuCw
Moss
Rootw
(b)
Abandoned channels, beneath SR
Abandoned channels, outside SR
Active channels, beneath SR
Active channels, outside SR
SOCtot (kg m-3 soil)
27.0
23.5
20.0
16.5
13.0
0.20
0.45
0.70
0.95
1.20
LAIw (m2 m-2 soil)
(c)
SOCtot (kg m-3 soil)
22.0
19.5
17.0
14.5
12.0
OWi
OWo
YWi
YWo
0
18
36
54
72
TLNw (g m-2 soil)
(d)
Fisher's C = 1.72
df = 4, P = 0.79
SOCtot
rm2 = 0.41
0.86
-0.64
LAIw
rm2 = 0.62
0.34
TLNw
rm2 = 0.43
0.79
0.55
0.12
0.40
Salix richardsonii
(outside vs beneath patches)
Hydrological regime
(active vs abandoned channels)

Figure 5

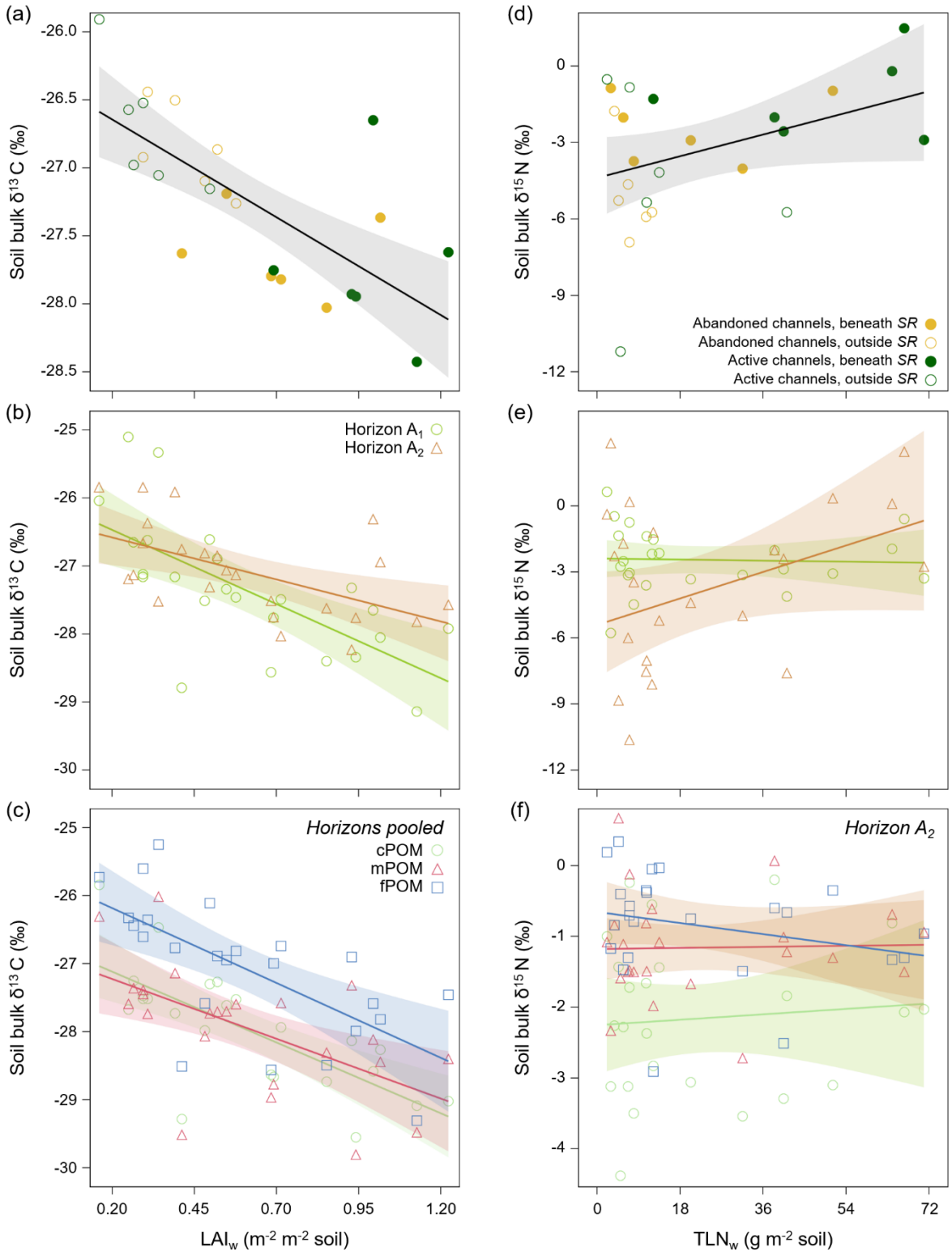
(a)
(b)
(c)
(d)
(e)
(f)
Soil bulk δ13 C (‰)
Soil bulk δ15 N (‰)
Horizon A1
Horizon A2
Horizons pooled
cPOM
mPOM
fPOM
Abandoned channels, beneath SR
Abandoned channels, outside SR
Active channels, beneath SR
Active channels, outside SR
LAIw (m-2 m-2 soil)
TLNw (g m-2 soil)

Figure 6

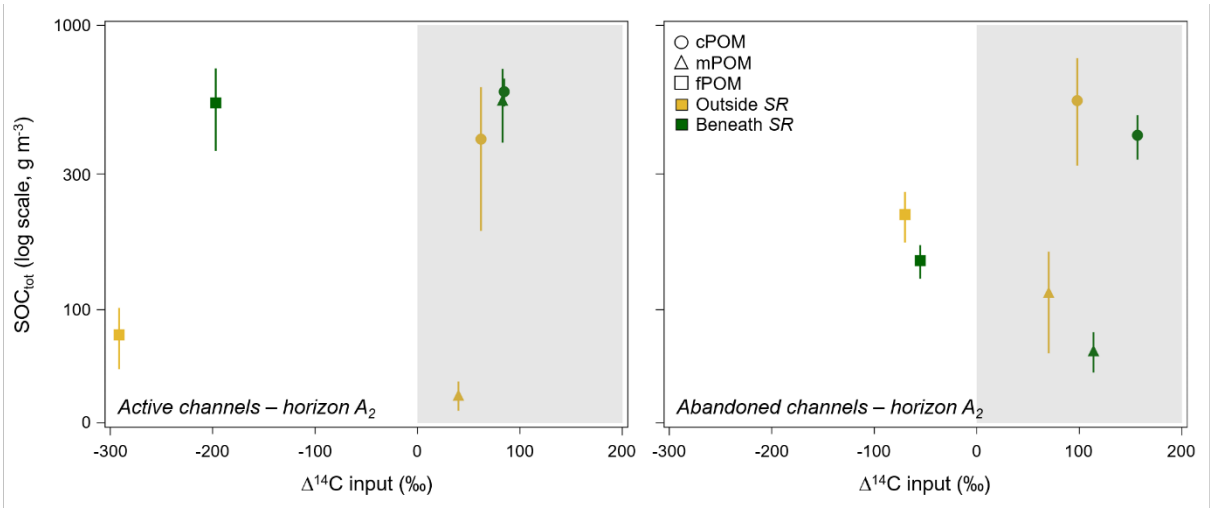
1000
300
100
0
SOC$_{tot}$ (log scale, g m^{-3})
Active channels – horizon A_2
-300
-200
-100
0
100
200
Δ^{14}C input (‰)
cPOM
mPOM
fPOM
Outside SR
Beneath SR
Abandoned channels – horizon A_2
-300
-200
-100
0
100
200
Δ^{14}C input (‰)

Supplementary material 1. Mean (± 1 SE) values of response variables in plots located outside and beneath *Salix richardsonii* (*SR*) patches along active and abandoned channels. n = 6 per vegetation condition per channel for each response variable. Test statistics are for fixed effects from linear mixed models. F-values in bold indicate significant effects, adjusted with the FDR procedure (see Supplementary Material 2). Measurement units are as follows: plant abundance in % cover, plant species richness in # species, leaf number in # leaves m^{-2}, leaf size in cm^2 $leaf^{-1}$, SLA_w in m^2 gDW^{-1} leaf, leaf nutrient content in 10^{-2} gNutrient gDW^{-1}, leaf C:N in gC gN^{-1}, root N content in 10^{-2} gN gDW^{-1}, surfacic (i.e. area based) soil organic carbon stocks (SOC) in kgC m^{-2} soil.

	Active channels			Abandoned channels			Channel			Vegetation			Channel x veg.	
	Outside *SR*	Beneath *SR*		Outside *SR*	Beneath *SR*		*df*	*F*		*df*	*F*		*df*	*F*
Plant community														
Salix richardsonii abundance	0.1 ± 0.1	54.2 ± 5.3		0.5 ± 0.4	66.3 ± 3.8		1	3.72		1	**341.79**		1	3.24
Graminoid abundance	0.0 ± 0.0	0.0 ± 0.0		0.1 ± 0.1	0.0 ± 0.0		1	0.96		1	1.04		1	0.96
Moss abundance	26.8 ± 15.6	9.6 ± 5.7		53.0 ± 14.8	32.5 ± 5.0		1	3.90		1	3.36		1	0.03
Species richness	5.5 ± 0.8	5.0 ± 1.0		6.5 ± 0.5	4.7 ± 0.7		1	0.14		1	3.68		1	1.20
Plant traits														
Leaf number	1313 ± 200	2821 ± 200		1546 ± 183	2475 ± 308		1	0.06		1	**28.58**		1	1.61
Leaf size	2.3 ± 0.0	3.5 ± 0.0		2.8 ± 0.1	2.9 ± 0.0		1	0.94		1	**90.63**		1	**79.11**
Specific leaf area (SLA_w)	75.7 ± 0.5	67.2 ± 0.2		71.1 ± 1.3	66.7 ± 0.0		1	12.26		1	**84.57**		1	8.05
Leaf C content	45.9 ± 0.2	44.5 ± 0.4		46.2 ± 0.3	44.3 ± 0.3		1	0.02		1	**76.93**		1	2.14
Leaf N content	2.8 ± 0.1	3.2 ± 0.1		2.6 ± 0.1	3.1 ± 0.1		1	1.53		1	**18.57**		1	0.65
Leaf P content	4.1 ± 0.3	5.5 ± 0.3		4.8 ± 0.5	6.1 ± 0.5		1	2.28		1	**11.44**		1	0.03
Leaf K content	16.3 ± 0.7	17.2 ± 0.7		16.0 ± 1.0	17.2 ± 1.1		1	0.03		1	1.24		1	0.03
Leaf Ca content	10.8 ± 0.8	12.7 ± 0.6		9.3 ± 0.6	12.7 ± 0.7		1	0.76		1	**38.66**		1	3.14
Leaf Mg content	3.7 ± 0.2	4.2 ± 0.1		3.8 ± 0.1	4.4 ± 0.4		1	0.25		1	**9.18**		1	0.08
Leaf nutrient content ($LNuC_w$)	37.8 ± 1.4	42.7 ± 1.4		36.5 ± 1.4	43.4 ± 1.4		1	0.05		1	**17.58**		1	0.48
Leaf C:N ratio	16.4 ± 0.7	14.2 ± 0.5		17.6 ± 0.3	14.3 ± 0.5		1	1.63		1	**27.89**		1	1.17
Root N content	1.3 ± 0.2	1.4 ± 0.1		1.7 ± 0.1	1.3 ± 0.1		1	1.02		1	1.57		1	3.89
Soil organic carbon stocks														
Surfacic SOC_{tot}	1.07 ± 0.08	1.48 ± 0.15		1.64 ± 0.06	1.55 ± 0.03		1	9.37		1	4.62		1	**11.36**
Surfacic SOC-A_1	0.31 ± 0.02	0.44 ± 0.11		0.66 ± 0.06	0.63 ± 0.05		1	12.47		1	0.85		1	1.77
Surfacic SOC-A_2	0.73 ± 0.10	0.99 ± 0.12		0.95 ± 0.07	0.87 ± 0.07		1	0.22		1	1.46		1	4.55
Surfacic C-cPOM	0.05 ± 0.02	0.08 ± 0.01		0.10 ± 0.02	0.12 ± 0.03		1	4.98		1	2.13		1	0.11
Surfacic C-mPOM	0.05 ± 0.01	0.13 ± 0.03		0.12 ± 0.02	0.13 ± 0.03		1	1.79		1	4.15		1	2.57
Surfacic C-fPOM	0.04 ± 0.01	0.12 ± 0.03		0.09 ± 0.02	0.11 ± 0.03		1	0.84		1	6.18		1	2.47
Surfacic C-cPOM-A_1	0.03 ± 0.01	0.05 ± 0.00		0.07 ± 0.01	0.10 ± 0.03		1	6.45		1	3.05		1	0.04
Surfacic C-cPOM-A_2	0.02 ± 0.01	0.03 ± 0.00		0.03 ± 0.01	0.02 ± 0.00		1	0.07		1	0.04		1	1.02
Surfacic C-mPOM-A_1	0.05 ± 0.01	0.09 ± 0.02		0.11 ± 0.02	0.13 ± 0.03		1	3.18		1	2.54		1	0.88
Surfacic C-mPOM-A_2	0.00 ± 0.00	0.03 ± 0.01		0.01 ± 0.00	0.00 ± 0.00		1	6.27		1	7.37		1	**10.61**
Surfacic C-fPOM-A_1	0.04 ± 0.01	0.09 ± 0.03		0.08 ± 0.02	0.10 ± 0.03		1	1.79		1	3.44		1	0.47
Surfacic C-fPOM-A_2	0.00 ± 0.00	0.03 ± 0.01		0.01 ± 0.00	0.01 ± 0.00		1	1.92		1	5.25		1	**9.39**

Supplementary material 2. False Discovery Rate (FDR) procedure applied on variables used in linear mixed models testing the effect of hydrological regime and *Salix richardsonii* (*SR*) occurrence on plant communities and soil conditions (c.f. Table 1 and Supplementary material 1). The procedure was applied separately for each of the fixed factors, i.e. channel (active vs abandoned), vegetation condition (outside vs beneath *S. richardsonii*), and the interaction between channel and vegetation condition. Values in bold indicate significant effects after the FDR procedure was applied. In the FDR procedure, the significant threshold is set at the highest *P*-value at which the inequality $P \leq q$ holds true, with this and all smaller *P*-values corresponding to significant comparisons (Benjamini and Hochberg 1995; but see Pike 2011 for the method applied in ecology and evolution). Here, q = (*P*rank/number of tests)*0.05.

	Channel				Vegetation				Channel x vegetation		
	P	*rank*	*q*		*P*	*rank*	*q*		*P*	*rank*	*q*
Plant community				*Plant community*				*Plant community*			
SR abundance	0.083	1	0.013	***SR* abundance**	**<.0001**	**1**	**0.013**	*SR* abundance	0.102	1	0.013
Moss abundance	0.077	2	0.025	Species richness	0.084	2	0.025	Species richness	0.298	2	0.025
Graminoid abundance	0.350	3	0.038	Moss abundance	0.097	3	0.038	Graminoid abundance	0.350	3	0.038
Species richness	0.718	4	0.050	Graminoid abundance	0.332	4	0.050	Moss abundance	0.874	4	0.050
Plant traits				*Plant traits*				*Plant traits*			
Moss biomass	**0.0003**	**1**	**0.002**	**Total abg biomass**	**<.0001**	**1**	**0.002**	**Leaf size**	**<.0001**	**1**	**0.002**
SLA_w	0.006	2	0.004	**Shrub abg biomass**	**<.0001**	**2**	**0.004**	**LAI_w**	**0.001**	**2**	**0.004**
Shrub leaf biomass	0.069	3	0.006	**Shrub shoot biomass**	**<.0001**	**3**	**0.006**	SLA_w	0.018	3	0.006
TLN_w	0.086	4	0.008	**LAI_w**	**<.0001**	**4**	**0.008**	Root N content	0.077	4	0.008
Total abg biomass	0.106	5	0.010	**Leaf size**	**<.0001**	**5**	**0.010**	Leaf Ca content	0.107	5	0.010
Leaf P content	0.162	6	0.013	**SLA_w**	**<.0001**	**6**	**0.013**	Leaf $\delta^{15}N$	0.140	6	0.013
Leaf $\delta^{13}C$	0.198	7	0.015	**Leaf C content**	**<.0001**	**7**	**0.015**	Graminoid abg biomass	0.152	7	0.015
Graminoid abg biomass	0.227	8	0.017	**Leaf Ca content**	**<.0001**	**8**	**0.017**	Leaf C content	0.174	8	0.017
Leaf C:N ratio	0.231	9	0.019	**Total plant biomass**	**0.0002**	**9**	**0.019**	Leaf number	0.233	9	0.019
Leaf N content	0.244	10	0.021	**Leaf number**	**0.0003**	**10**	**0.021**	Shrub leaf biomass	0.240	10	0.021
LAI_w	0.278	11	0.023	**Leaf C:N ratio**	**0.0004**	**11**	**0.023**	Shrub shoot biomass	0.245	11	0.023
Root N content	0.336	12	0.025	**Leaf N content**	**0.002**	**12**	**0.025**	TLN_w	0.291	12	0.025
Leaf size	0.355	13	0.027	**$LNuC_w$**	**0.002**	**13**	**0.027**	Leaf C:N ratio	0.306	13	0.027
Shrub shoot biomass	0.393	14	0.029	**TLN_w**	**0.006**	**14**	**0.029**	Shrub abg biomass	0.349	14	0.029
Leaf Ca content	0.403	15	0.031	**Leaf P content**	**0.007**	**15**	**0.031**	Total abg biomass	0.369	15	0.031
Shrub abg biomass	0.581	16	0.033	**Shrub leaf biomass**	**0.009**	**16**	**0.033**	Leaf N content	0.438	16	0.033
Leaf Mg content	0.625	17	0.035	**Leaf Mg content**	**0.013**	**17**	**0.035**	$LNuC_w$	0.506	17	0.035
Leaf number	0.811	18	0.038	Graminoid abg biomass	0.052	18	0.038	Root biomass	0.544	18	0.038
$LNuC_w$	0.834	19	0.040	Leaf $\delta^{15}N$	0.079	19	0.040	Moss biomass	0.621	19	0.040
Leaf K content	0.857	20	0.042	Leaf $\delta^{13}C$	0.115	20	0.042	Leaf $\delta^{13}C$	0.679	20	0.042
Total plant biomass	0.864	21	0.044	Root biomass	0.136	21	0.044	Total plant biomass	0.702	21	0.044
Root biomass	0.883	22	0.046	Root N content	0.239	22	0.046	Leaf Mg content	0.780	22	0.046
Leaf C content	0.901	23	0.048	Leaf K content	0.292	23	0.048	Leaf K content	0.857	23	0.048

Leaf $\delta^{15}N$	0.939	24	0.050		Moss biomass	0.621	24	0.050		Leaf P content	0.864	24	0.050
Soil conditions					*Soil conditions*					*Soil conditions*			
FDD	**0.001**	**1**	**0.005**		Horizon A_1 depth	0.083	1	0.005		Soil total N content	0.023	1	0.005
pH	**0.011**	**2**	**0.010**		Thaw front depth	0.190	2	0.010		pH	0.047	2	0.010
Total water content	**0.013**	**3**	**0.015**		TDD	0.262	3	0.015		Soil C:N ratio	0.102	3	0.015
TDD	**0.020**	**4**	**0.020**		Soil total N content	0.276	4	0.020		Thaw front depth	0.115	4	0.020
Horizon A_1 depth	0.038	5	0.025		Soil C:N ratio	0.327	5	0.025		Horizon A_2 depth	0.175	5	0.025
Thaw front depth	0.109	6	0.030		pH	0.433	6	0.030		FDD	0.218	6	0.030
Soil C:N ratio	0.155	7	0.035		FDD	0.457	7	0.035		Horizon A_1 depth	0.335	7	0.035
Soil bulk density	0.527	8	0.040		Horizon A_2 depth	0.626	8	0.040		TDD	0.369	8	0.040
Horizon A_2 depth	0.595	9	0.045		Total water content	0.733	9	0.045		Soil bulk density	0.801	9	0.045
Soil total N content	0.642	10	0.050		Soil bulk density	0.774	10	0.050		Total water content	0.857	10	0.050
Volumetric SOC stocks					*Volumetric SOC stocks*					*Volumetric SOC stocks*			
C-mPOM-A_2	0.033	1	0.004		C-mPOM-A_2	0.021	1	0.004		C-mPOM-A_2	0.009	1	0.004
C-cPOM	0.161	2	0.008		SOC-A_1	0.021	2	0.008		C-fPOM-A_2	0.010	2	0.008
C-fPOM-A_2	0.223	3	0.013		C-fPOM	0.023	3	0.013		SOC_{tot}	0.059	3	0.013
SOC_{tot}	0.305	4	0.017		C-fPOM-A_2	0.042	4	0.017		SOC-A_2	0.074	4	0.017
C-mPOM	0.378	5	0.021		C-mPOM	0.090	5	0.021		C-mPOM	0.131	5	0.021
SOC-A_2	0.437	6	0.025		SOC_{tot}	0.110	6	0.025		C-fPOM	0.131	6	0.025
C-fPOM	0.623	7	0.029		C-cPOM	0.150	7	0.029		SOC-A_1	0.317	7	0.029
C-fPOM-A_1	0.624	8	0.033		SOC-A_2	0.189	8	0.033		C-cPOM-A_2	0.341	8	0.033
SOC-A_1	0.628	9	0.038		C-cPOM-A_1	0.406	9	0.038		C-fPOM-A_1	0.686	9	0.038
C-mPOM-A_1	0.725	10	0.042		C-mPOM-A_1	0.688	10	0.042		C-cPOM	0.843	10	0.042
C-cPOM-A_2	0.931	11	0.046		C-fPOM-A_1	0.860	11	0.046		C-cPOM-A_1	0.990	11	0.046
C-cPOM-A_1	0.953	12	0.050		C-cPOM-A_2	0.871	12	0.050		C-mPOM-A_1	0.997	12	0.050
Surfacic SOC stocks					*Surfacic SOC stocks*					*Surfacic SOC stocks*			
SOC-A_1	0.005	1	0.004		C-mPOM-A_2	0.022	1	0.004		**SOC_{tot}**	**0.007**	**1**	**0.004**
SOC_{tot}	0.012	2	0.008		C-fPOM	0.032	2	0.008		**C-mPOM-A_2**	**0.009**	**2**	**0.008**
C-cPOM-A_1	0.029	3	0.013		C-fPOM-A_2	0.045	3	0.013		**C-fPOM-A_2**	**0.012**	**3**	**0.013**
C-mPOM-A_2	0.031	4	0.017		SOC_{tot}	0.057	4	0.017		SOC-A_2	0.059	4	0.017
C-cPOM	0.050	5	0.021		C-mPOM	0.069	5	0.021		C-mPOM	0.140	5	0.021
C-mPOM-A_1	0.105	6	0.025		C-fPOM-A_1	0.093	6	0.025		C-fPOM	0.147	6	0.025
C-fPOM-A_2	0.196	7	0.029		C-cPOM-A_1	0.111	7	0.029		SOC-A_1	0.213	7	0.029
C-mPOM	0.210	8	0.033		C-mPOM-A_1	0.142	8	0.033		C-cPOM-A_2	0.336	8	0.033
C-fPOM-A_1	0.211	9	0.038		C-cPOM	0.175	9	0.038		C-mPOM-A_1	0.371	9	0.038
C-fPOM	0.380	10	0.042		SOC-A_2	0.255	10	0.042		C-fPOM-A_1	0.508	10	0.042
SOC-A_2	0.648	11	0.046		SOC-A_1	0.378	11	0.046		C-cPOM	0.747	11	0.046
C-cPOM-A_2	0.793	12	0.050		C-cPOM-A_2	0.842	12	0.050		C-cPOM-A_1	0.844	12	0.050

Reference

Pike N. 2011. Using false discovery rates for multiple comparisons in ecology and evolution. Methods in Ecology and Evolution 2: 278-282.

Supplementary material 3. Mean species richness and mean species cover of vascular and non-vascular taxa found in plots located outside and beneath *Salix richardsonii* (*SR*) patches along active and abandoned channels. Species richness and species abundance were estimated within a 0.7 m x 0.7 m quadrat arranged in each of the 24 sampled vegetation plots. < for cover < 0.1% and << for cover < 0.01%. Species names are reported according to the Database of Vascular Plants of Canada (VASCAN; https://data.canadensys.net/vascan/search).

	Active channels			Abandoned channels	
	Outside *SR*	Beneath *SR*		Outside *SR*	Beneath *SR*
Mean species richness	6	5		7	5
Plant species cover (%)					
Caryophyllaceae					
Stellaria longipes Goldie	<<	0		0	0
Equisetaceae					
Equisetum arvense L.	0.6	<<		<	<<
Fabaceae					
Astragalus alpinus L.	0.4	<<		1.8	<<
Juncaceae					
Luzula nivalis Spreng.	<<	0		0.4	0
Poaceae					
Alopecurus magellanicus Lam.	<	0		0	0
Arctagrostis latifolia (R. Br.) Griseb.	0.5	<		0.2	<
Poa arctica R. Br.	<<	0		0	0
Other spp.	<<	0		<	0
Polygonaceae					
Bistorta vivipara (L.) Delarbre	<<	<		<<	<<
Rosaceae					
Dryas integrifolia Vahl	0.5	<		0.9	0
Salicaceae					
Salix richardsonii Hooker	<	54.2		0.5	66.3
Salix arctica Pall.	3.3	<<		5.8	0.2
Salix reticulata L.	0.6	0		2.2	<
Lichens					
Peltigera spp.	0	0.4		0	0.4
Stereocaulon spp.	0	0.4		0	1.2
Other spp.	0	0		0.5	0
Mosses	26.8	9.6		53.0	32.5
Cryptogamic crust cover (%)	64.6	6.3		25.0	0
Litter cover (%)	3.1	41.7		5.8	45.8
Standing dead cover (%)	0.5	0		0.6	0

Supplementary material 4. (a) Canonical correspondence analysis testing the association between plant community and soil conditions (i.e. thaw front depth, bulk density, water content, pH, freezing degree-days, thawing degree-days, C:N ratio, and total N content). (b) Principal component analysis of plots located outside and beneath *Salix richardsonii* (*SR*) patches in active and abandoned channels, relative to leaf nutrients (i.e. C/N/P/K/Ca/Mg content, C:N ratio, ^{13}C and ^{15}N composition) of *Salix* spp.

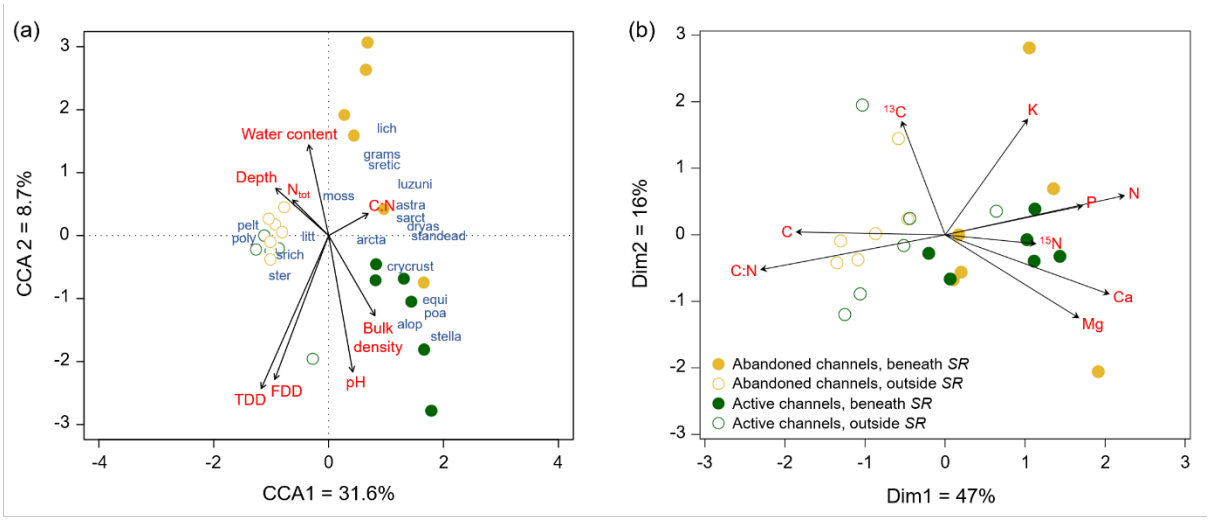

Supplementary material 5. Plant biomass (a,b) and soil conditions (c-f) in plots located outside and beneath *Salix richardsonii* (*SR*) patches along active and abandoned channels. n = 6 per vegetation condition per channel for each response variable, except for soil total water content (n = 12) and soil freezing/thawing degree-days (FDD/TDD; n = 3).

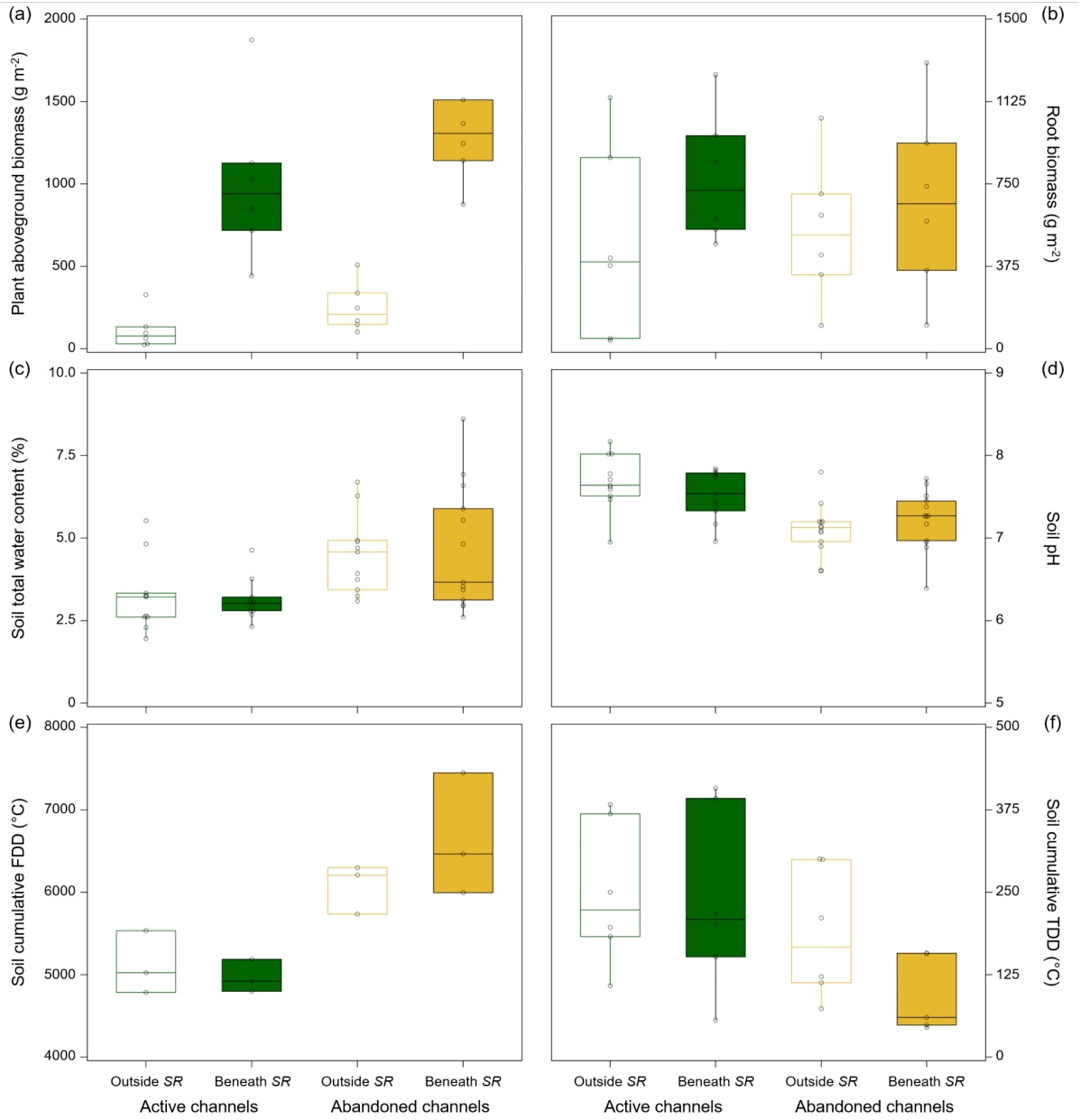

Supplementary material 6. Surfacic (i.e. area based) soil organic carbon (SOC, kg m^{-2}) outside and beneath *Salix richardsonii* (*SR*) patches located along active and abandoned channels. Panel (a) refers to total SOC (SOC_{tot}), while panels (b) and (c) represent SOC content per horizon and OM compartment ($n = 6$ per vegetation condition per channel). The particulate organic matter compartments were discriminated as follows: coarse organic matter (cPOM, 2 mm to 1 mm), medium organic matter (mPOM, 1 mm to 250 µm) and fine organic matter (fPOM, 250 µm to 63 µm). The mineral-associated OM compartment (MAOM), estimated as the difference between SOC_{tot} and SOC of the three measured POM compartments, is also represented. See Supplementary material 1 for corresponding statistics. *$P < 0.05$, †$P < 0.1$.

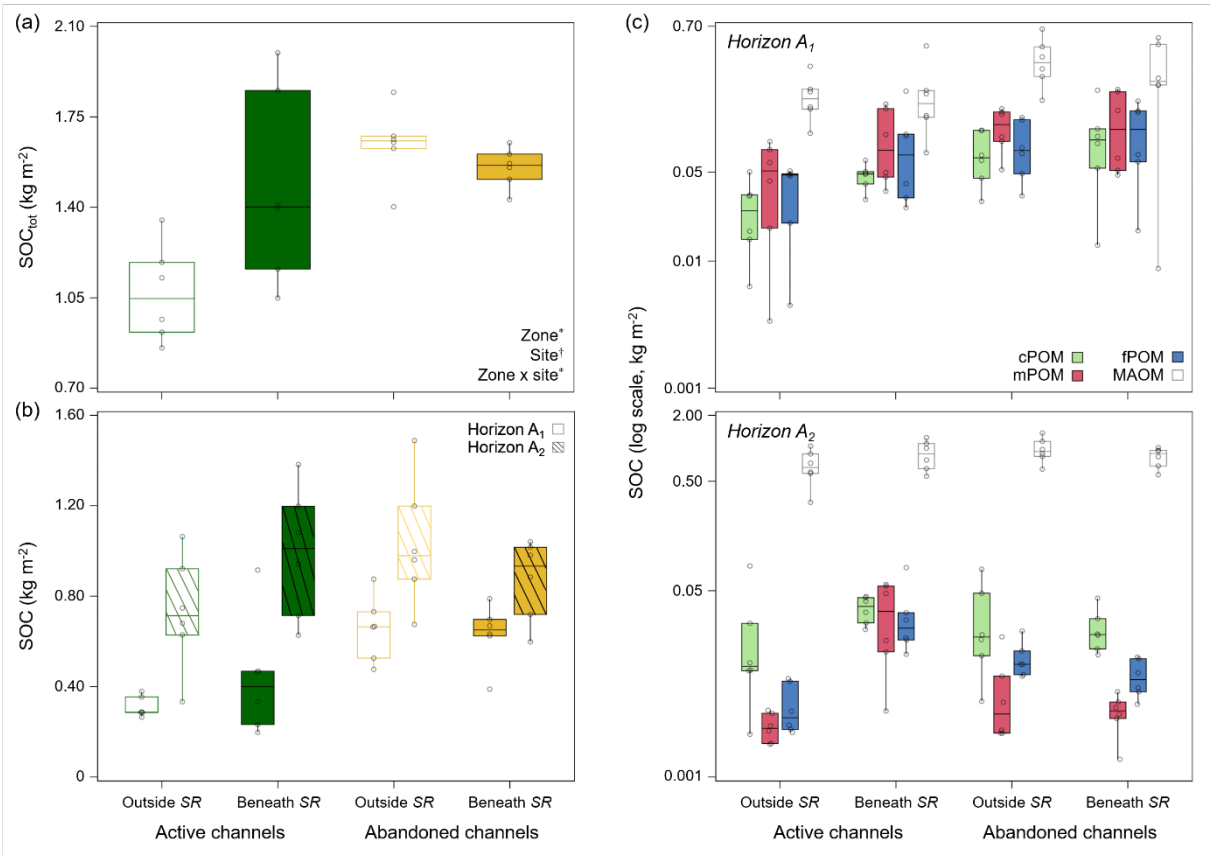

Supplementary material 7. $\delta^{13}C$, $\delta^{15}N$ and C:N ratio of plant leaves, plant roots and OM compartments found in soil horizons A_1 and A_2 sampled in plots located outside and beneath *Salix richardsonii* (*SR*) patches along active and abandoned channels. The particulate organic matter compartments were discriminated as follows: coarse organic matter (cPOM, 2 mm to 1 mm), medium organic matter (mPOM, 1 mm to 250 µm) and fine organic matter (fPOM, 250 µm to 63 µm).